

University of Windsor

Scholarship at UWindor

Electronic Theses and Dissertations

Theses, Dissertations, and Major Papers

1-1-1970

Collisional excitation transfer and quenching in vapours of potassium and rubidium.

Eugene S. Hrycyshyn
University of Windsor

Follow this and additional works at: <https://scholar.uwindsor.ca/etd>

Recommended Citation

Hrycyshyn, Eugene S., "Collisional excitation transfer and quenching in vapours of potassium and rubidium." (1970). *Electronic Theses and Dissertations*. 6082.
<https://scholar.uwindsor.ca/etd/6082>

This online database contains the full-text of PhD dissertations and Masters' theses of University of Windsor students from 1954 forward. These documents are made available for personal study and research purposes only, in accordance with the Canadian Copyright Act and the Creative Commons license—CC BY-NC-ND (Attribution, Non-Commercial, No Derivative Works). Under this license, works must always be attributed to the copyright holder (original author), cannot be used for any commercial purposes, and may not be altered. Any other use would require the permission of the copyright holder. Students may inquire about withdrawing their dissertation and/or thesis from this database. For additional inquiries, please contact the repository administrator via email (scholarship@uwindsor.ca) or by telephone at 519-253-3000ext. 3208.

COLLISIONAL EXCITATION TRANSFER AND QUENCHING

IN VAPOURS OF POTASSIUM AND RUBIDIUM

by

Eugene S. Hrycyshyn

A Thesis

Submitted to the Faculty of Graduate Studies through the Department
of Physics in Partial Fulfillment of the Requirements for
the Degree of Doctor of Philosophy at the
University of Windsor

Windsor, Ontario

1970

UMI Number: DC52650

INFORMATION TO USERS

The quality of this reproduction is dependent upon the quality of the copy submitted. Broken or indistinct print, colored or poor quality illustrations and photographs, print bleed-through, substandard margins, and improper alignment can adversely affect reproduction.

In the unlikely event that the author did not send a complete manuscript and there are missing pages, these will be noted. Also, if unauthorized copyright material had to be removed, a note will indicate the deletion.

UMI[®]

UMI Microform DC52650

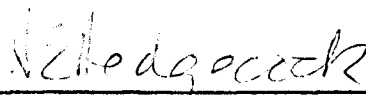
Copyright 2008 by ProQuest LLC.

All rights reserved. This microform edition is protected against unauthorized copying under Title 17, United States Code.

ProQuest LLC
789 E. Eisenhower Parkway
PO Box 1346
Ann Arbor, MI 48106-1346

1947

APPROVED BY:



Dr. N. E. Hedgecock (Chairman)



Dr. M. Czajkowski



Dr. A. van Wijngaarden

321913

ABSTRACT

The method of sensitized fluorescence was used to determine cross sections for the various excitation transfer processes occurring in K - Rb vapour mixtures and for $^2P_{1/2} \leftrightarrow ^2P_{3/2}$ mixing and $^2S_{1/2} - ^2P_{1/2}, ^2P_{3/2}$ quenching in rubidium induced in collisions with several diatomic and polyatomic molecules in their ground states. The alkali vapour in the fluorescence cell, which was kept at low pressures to avoid serious effects of radiation imprisonment, was irradiated by one component of the appropriate resonance doublet. The resulting fluorescence, which consisted of the wavelength component present in the exciting light (resonance fluorescence) and those components which arose from the emission by atoms collisionally populated (sensitized fluorescence), was resolved and observed at right angles to the direction of the incident beam. Measurements of sensitized-to-resonance fluorescent intensity ratios in relation to rubidium vapour pressure yielded the following cross sections for excitation transfer in K - Rb vapour mixtures:

$$Q_{12}, (K^4^2P_{1/2} \rightarrow Rb^5^2P_{3/2}) = 40 \text{ \AA}^2, \quad Q_{22}, (K^4^2P_{3/2} \rightarrow Rb^5^2P_{3/2}) = 27 \text{ \AA}^2,$$

$$Q_{11}, (K^4^2P_{1/2} \rightarrow Rb^5^2P_{1/2}) = 2.7 \text{ \AA}^2, \quad Q_{21}, (K^4^2P_{3/2} \rightarrow Rb^5^2P_{1/2}) = 1.9 \text{ \AA}^2,$$

$$Q_{12}'', (K^4^2P_{1/2} \rightarrow K^4^2P_{3/2}) = 260 \text{ \AA}^2, \quad \text{and} \quad Q_{21}'', (K^4^2P_{1/2} \leftarrow K^4^2P_{3/2}) = 175 \text{ \AA}^2.$$

In mixtures of rubidium with molecular gases, measurements of the intensity ratios in relation to gas pressures gave the following cross sections for the mixing and quenching collisions. For H_2 :

$$\begin{aligned}
Q_{12}(^2P_{1/2} - ^2P_{3/2}) &= 11 \text{ \AA}^2, \quad Q_{21}(^2P_{1/2} - ^2P_{3/2}) = 15 \text{ \AA}^2, \quad Q_{10}(^2S_{1/2} - \\
^2P_{1/2}) &= 6 \text{ \AA}^2, \quad Q_{20}(^2S_{1/2} - ^2P_{3/2}) = 3 \text{ \AA}^2; \text{ for HD: } Q_{12} = 18 \text{ \AA}^2, \\
Q_{21} &= 25 \text{ \AA}^2, \quad Q_{10} = 6 \text{ \AA}^2, \quad Q_{20} = 5 \text{ \AA}^2; \text{ for D}_2: \quad Q_{12} = 22 \text{ \AA}^2, \quad Q_{21} = \\
30 \text{ \AA}^2, \quad Q_{10} &= 3 \text{ \AA}^2, \quad Q_{20} = 5 \text{ \AA}^2; \text{ for N}_2: \quad Q_{12} = 16 \text{ \AA}^2, \quad Q_{21} = 23 \text{ \AA}^2, \\
Q_{10} &= 58 \text{ \AA}^2, \quad Q_{20} = 43 \text{ \AA}^2; \text{ for CH}_4: \quad Q_{12} = 30 \text{ \AA}^2, \quad Q_{21} = 42 \text{ \AA}^2; \\
\text{for CD}_4: \quad Q_{12} &= 28 \text{ \AA}^2, \quad Q_{21} = 38 \text{ \AA}^2; \text{ for C}_2\text{H}_4: \quad Q_{12} = 23 \text{ \AA}^2, \quad Q_{21} = \\
32 \text{ \AA}^2, \quad Q_{10} &= 139 \text{ \AA}^2, \quad Q_{20} = 95 \text{ \AA}^2; \text{ for C}_2\text{H}_6: \quad Q_{12} = 57 \text{ \AA}^2, \text{ and} \\
Q_{21} &= 77 \text{ \AA}^2.
\end{aligned}$$

ACKNOWLEDGEMENTS

I wish to thank Dr. L. Krause for his support and guidance throughout the course of this research and for his constructive criticism of the original manuscript. I am also grateful to the members of the Atomic Physics Group with whom I have had many informative discussions.

Acknowledgements are due to Mr. A. Buzzeo who prepared most of the diagrams, Mr. W. Eberhart who constructed the fluorescence cell and the glass vacuum system, and Mr. W. Grewe who manufactured the cryostat and other essential pieces of apparatus. I am grateful to Mrs. M. Ridsdale for her proficient typing of this dissertation.

The financial assistance which I have received from the Province of Ontario and the National Research Council of Canada has been greatly appreciated.

TABLE OF CONTENTS

	Page
ABSTRACT	iii
ACKNOWLEDGEMENTS	v
LIST OF TABLES	viii
LIST OF FIGURES	ix
I. INTRODUCTION	1
II. MACROSCOPIC THEORY OF THE INELASTIC PROCESSES	7
A. Collisions Between Excited Potassium Atoms and Ground State Rubidium Atoms	7
B. Collisions Between Excited Rubidium Atoms and Ground State Diatomic or Polyatomic Molecules	13
C. Calculation of the Cross Sections	18
III. DESCRIPTION OF THE APPARATUS	20
IV. EXPERIMENTAL PROCEDURE	27
V. SENSITIZED FLUORESCENCE IN K - Rb VAPOUR MIXTURES	31
A. The Extinction Coefficients	31
B. The Cross Sections for K - Rb Collisions	33
(i) Energy Transfer from the 2P Substates of Potassium to the 2P Substates of Rubidium, Induced in Collisions with Ground State Rubidium Atoms	33
(ii) Mixing of the 2P Substates of Potassium Induced in Collisions with Ground State Rubidium Atoms	40
C. Discussion of the K - Rb Cross Sections	40

	Page
VI. SENSITIZED FLUORESCENCE AND QUENCHING INDUCED IN COLLISIONS OF RUBIDIUM ATOMS WITH MOLECULES	46
A. The Experimental Results	46
B. Discussion of the Results	52
VII. CONCLUSIONS	61
A. Transfer of Excitation in Potassium-Rubidium Collisions	61
B. Transfer of Excitation in Collisions Between Rubidium Atoms and Gas Molecules	62
C. Quenching of Rubidium Resonance Radiation by Collisions with Molecules	63
APPENDICES	65
A. Experimental Measurements of the Extinction Coefficients and Fluorescent Intensity Ratios in K - Rb Vapour Mixtures	65
B. Experimental Data for Rubidium - Molecular Gas Collisions	75
BIBLIOGRAPHY	85
VITA AUCTORIS	88

LIST OF TABLES

	Page
1. Cross Sections for Inelastic Collisions Between Excited Potassium and Ground State Rubidium Atoms	41
2. Cross Sections for Mixing and Quenching in Rb - Molecule Collisions	54
3. Cross Sections for Mixing and Quenching in Rb - H ₂ and Rb - N ₂ Systems	56

LIST OF FIGURES

	Page
1. Energy level diagram showing sensitized fluorescence in Rb induced by collisions with K atoms in their $4^2P_{3/2}$ states. The s coefficient denotes excitation by the absorption of photons, the $(\tau)^{-1}$ coefficients refer to spontaneous radiative decay and the Z coefficients to radiationless transfer of energy by inelastic collisions. The primary processes are represented by solid arrows.	8
2. Energy levels involved in sensitized fluorescence of Rb and in the quenching of the Rb resonance radiation induced by collisions with diatomic and polyatomic molecules.	15
3. Schematic arrangement of the apparatus.	21
4. The fluorescence cell with the ray diagram of the scheme used in the determinations of the extinction coefficients. A, entrance window; B, exit window; C, viewing window; D, side arm.	24
5. The variation with temperature of the extinction coefficients for the 7948 \AA component in pure rubidium vapour and in the potassium-rubidium vapour mixture.	32
6. A plot of the intensity ratio η_{12} , against temperature. The statistical errors are negligible.	34
7. A plot of the intensity ratio η_{22} , against temperature. The statistical errors are negligible.	35
8. A plot of the intensity ratio η_{11} , against temperature. (o) experimental results; (x) results corrected for reabsorption and trapping of resonance radiation. The error bars represent typical errors derived from counting statistics.	36
9. A plot of the intensity ratio η_{21} , against temperature. (o) experimental results; (x) results corrected for reabsorption and trapping of resonance radiation. The error bars represent typical errors derived from counting statistics.	37

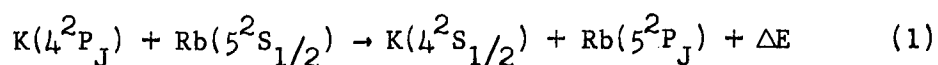
10. Plots of intensity ratios η and η' against partial pressure of rubidium vapour. (*) η_1 ; (Δ) η_1' ; (\diamond) η_2 ; (o) η_2' . The errors arising from counting statistics are too small to be shown. 42
11. Plots of intensity ratios η_1 and η_2 against H_2 , HD and D_2 gas pressures. (o) D_2 ; (\square) HD ; (Δ) H_2 . 47
12. Plots of intensity ratios η_1 and η_2 against H_2 , HD and D_2 gas pressures. (o) D_2 ; (\square) HD ; (Δ) H_2 . 48
13. Plots of intensity ratios η_1 and η_2 against C_2H_6 , CH_4 and CD_4 gas pressures. (o) C_2H_6 ; (\square) CH_4 ; (Δ) CD_4 . 49
14. Plots of intensity ratios η_1 and η_2 against N_2 and C_2H_4 gas pressures. 50
15. Plots of collision numbers Z_{12} , Z_{21} , Z_{10} , Z_{20} , and the coefficients A and D against HD pressure. The dashed lines Z_{12} and Z_{21} are extrapolations of the straight lines obtained for A and D at low gas pressures where quenching is negligible ($Z_{21} = A$, $Z_{12} = D$). 51
16. Plots of collision numbers Z_{12} , Z_{21} , Z_{10} , Z_{20} , and the coefficients A and D against N_2 pressure. The dashed lines Z_{12} and Z_{21} are extrapolations of the straight lines obtained for A and D at low gas pressures where quenching is negligible ($Z_{21} = A$, $Z_{12} = D$). 53

I. INTRODUCTION

The understanding of the physical behaviour of systems such as flames, discharges, stellar atmospheres, the aurora and others, where atoms and molecules are continuously excited and de-excited by the absorption and emission of radiation and by collisions with other atoms, molecules and electrons, requires a detailed knowledge of the reaction rates or cross sections for the various processes that are involved. Much interest has been devoted recently to all such processes, among which inelastic collisions leading to the transfer of excitation energy in heavy atoms, have been receiving particular attention in this laboratory. Collisions involving alkali metals, because of their relatively simple hydrogen-like structure, are especially interesting since some comparison between theory and experiment is possible. Of these, alkali - inert gas collisions and collisions between identical alkali atoms have been investigated most thoroughly. Theoretical studies have had some success in predicting cross sections for the collisional transfer of excitation between the resonance states of alkali atoms when the energy separations between the resonance states are small and can be neglected, as is the case with sodium (Callaway and Bauer 1965). However, in collisions involving atoms such as rubidium and cesium, where the energy gaps between the fine-structure substates are large and consequently cannot be neglected, agreement within an order of magnitude between

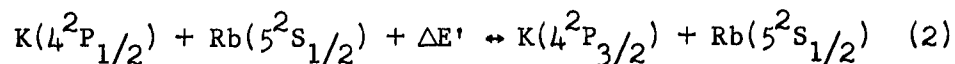
theory and experiment has been achieved only very recently (Dashevskaya et al, 1970). It is the purpose of this research to study inelastic collision processes in which excitation energy is transferred between atomic substates of relatively large energy separations. Specifically, cross sections were measured for the collision processes occurring in mixtures of potassium and rubidium vapours and of rubidium with molecular gases.

When a mixture of potassium and rubidium vapours is irradiated with one component of the potassium resonance doublet, the resulting fluorescence includes the wavelength component present in the incident light (resonance fluorescence) as well as those components which arise as a result of collisional excitation transfer (sensitized fluorescence). The processes of excitation transfer from the potassium to the rubidium atoms may be represented by the following general equation:



where $J = 1/2$ or $3/2$ and ΔE is the energy defect between the appropriate potassium and rubidium states, which is converted into relative kinetic energy of the colliding atoms. The reverse processes in which the energy ΔE is supplied by the kinetic energy of the colliding partners is not shown here since the low fluorescent intensities made observation of these events impossible. Collisions of excited potassium atoms with ground state rubidium atoms may also lead to a transfer of excitation energy between the potassium resonance states. These processes, usually referred to as collisional mixing, may be

represented by the following equation:



where $\Delta E'$ is the energy defect between the $4^2P_{1/2}$ and $4^2P_{3/2}$ states of potassium and equals 57 cm^{-1} . Both the forward and reverse processes could be observed.

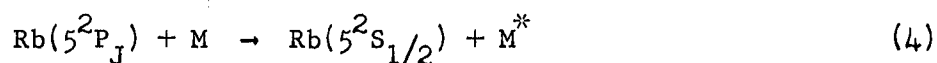
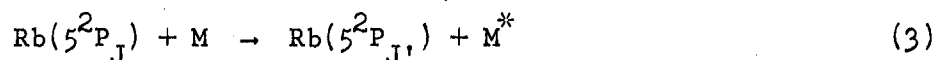
Some other recent investigations of sensitized fluorescence induced in collisions between two dissimilar metallic atoms and leading to absolute cross sections for excitation transfer, have been carried out with mixtures of sodium and mercury (Kraulinya 1964), mercury and thalium (Kraulinya and Lezdin 1966; Hudson and Curnutte 1966), mercury and zinc (Sosinskii and Morosov 1965), and cadmium and cesium (Friedrich and Seiwert 1957). An earlier study of a system containing two alkali metals at low vapour densities has been reported by Czajkowski, McGillis and Krause (1966b), who obtained total cross sections for inelastic collisions between excited rubidium and ground state cesium atoms. Thangaraj (1948) also estimated the cross section for inelastic collisions between potassium and rubidium atoms at relatively high vapour densities, and Seiwert (1956) studied a sodium - potassium mixture under similar conditions, though he did not obtain any collision cross sections. Since the publication of the results of this investigation (Hrycyshyn and Krause 1969ab), cross sections for excitation transfer from potassium to rubidium atoms have been reported by other authors (Ornstein and Zare 1969; Stacey and Zare 1970).

The study of excitation transfer between the rubidium 2P_J fine structure substates (collisional mixing) induced in collisions

with molecular gases, is of interest because the results of a previous study (McGillis and Krause 1968b, 1969) showed that cross sections for mixing of the 2P_J substates of cesium which are separated by an energy gap of 554 cm^{-1} , induced in collisions with diatomic and some polyatomic molecules, were about five orders of magnitude larger than the corresponding cross sections for collisions with inert gas atoms (Czajkowski, McGillis and Krause 1966a). On the other hand, mixing cross sections observed in sodium ($\Delta E = 17.2 \text{ cm}^{-1}$) collisions with inert gases (Pitre and Krause 1967) are of the same order of magnitude as the corresponding cross sections observed in mixtures of sodium and molecular gases (Stupavsky and Krause 1968, 1969). It is apparent that in collisions with molecules, the transfer of excitation energy between the 2P_J substates of the alkali atoms would be greatly enhanced if the energy defect ΔE between these states could be transferred into molecular vibrational and rotational levels as well as into the kinetic energies of the colliding partners. However, little is known of the effects of internal molecular structure, especially those of rotational excitation on the various collisional processes.

In this investigation, cross sections have been determined for inelastic collisions between excited rubidium atoms and various diatomic and polyatomic molecules leading to $5^2P_{1/2} \leftrightarrow 5^2P_{3/2}$ mixing. The energy separation between these resonance levels in rubidium equals 238 cm^{-1} , making the interaction considerably less adiabatic than in the case of cesium where the resonance defect amounts to 554 cm^{-1} . Molecules are also known to be efficient in collisionally deactivating (quenching) excited states (Mitchell and Zemansky 1961). Since the

effects of quenching can be separated from those of mixing, the $5^2S_{1/2} \leftarrow 5^2P_{1/2}, 5^2P_{3/2}$ quenching cross sections could also be estimated. When a single component of the rubidium resonance doublet is used to irradiate the vapour-gas mixtures, the collisional processes which occur can be represented by the following equations:



where J and J' are either $1/2$ or $3/2$, and M^* represents a molecule whose translational, vibrational and rotational energy has changed as a result of collision. When $J \neq J'$, eq. (3) represents the excitation transfer process between the 2P_J states (mixing) and eq. (4) represents the quenching reaction.

The quenching of rubidium resonance radiation by various molecules has been recently studied at flame temperatures by Jenkins (1968), and Hooymayers and Nienhuis (1968) who reported the possibility of a resonance effect between the excited states in rubidium and the molecular vibrational levels. These authors did not attempt, however, to resolve the rubidium resonance doublet. If a resonance effect were present, the quenching cross sections of excited rubidium in collisions with molecules of a specific gas should be extremely sensitive as to which rubidium 2P_J substate would be initially excited. In this investigation, it was possible to obtain individual cross sections for the quenching of each 2P_J substate. It should be borne in mind, however, that if the quenching cross sections were strongly dependent

on the chemical properties of the molecules, a comparison of the results obtained at flame temperatures with those obtained in this experiment ($T = 340^{\circ}\text{K}$) might not be significant.

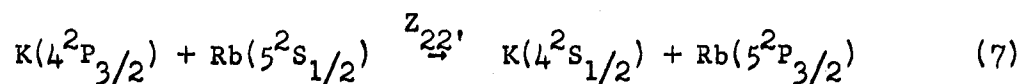
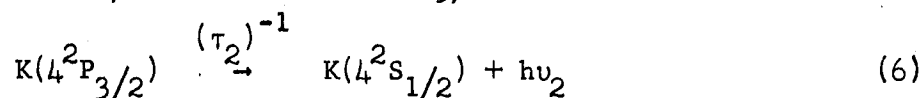
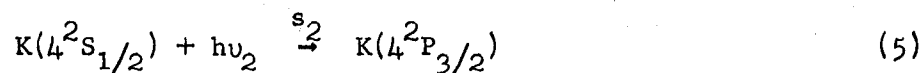
II. MACROSCOPIC THEORY OF THE INELASTIC PROCESSES

In order to experimentally determine the cross section for any specific process, it is first necessary to express it in terms of measurable quantities. Since the processes which occur in alkali - alkali collisions are not completely identical with those in alkali - molecular gas collisions where quenching reactions must be taken into account, each system will be treated separately.

A. Collisions Between Excited Potassium Atoms and Ground State Rubidium Atoms

The processes which occur when the potassium $4^2P_{3/2}$ state is optically excited in a K - Rb vapour mixture, are shown in Fig. 1. The most probable processes which give rise to resonance fluorescence and sensitized fluorescence are indicated by solid arrows; the broken arrows show reactions which also lead to sensitized fluorescence but are much less probable.

The various reactions are represented by the following equations:



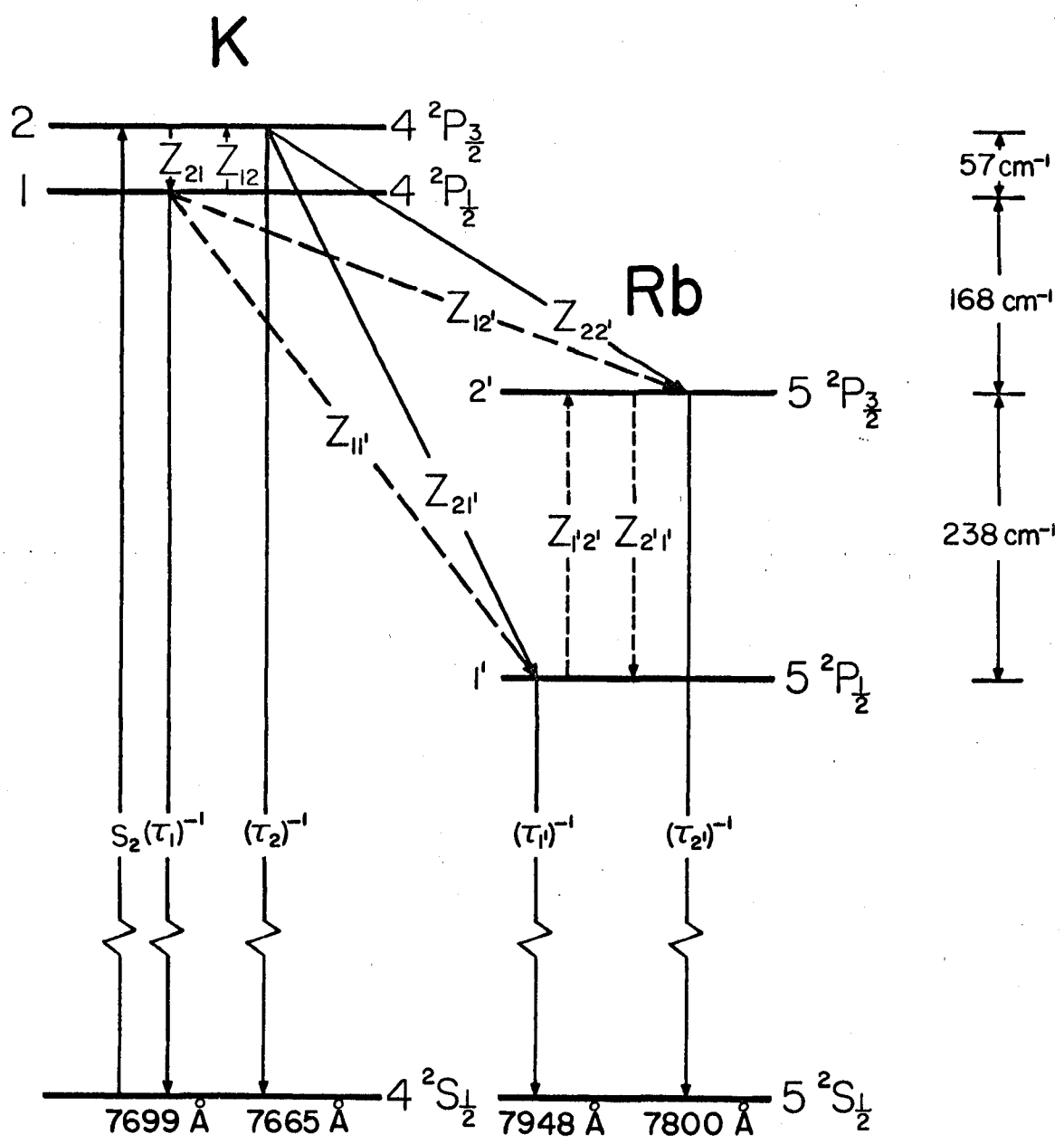


Fig. 1. Energy level diagram showing sensitized fluorescence in Rb induced by collisions with K atoms in their $4^2P_{3/2}$ states. The s^{-1} coefficient denotes excitation by the absorption of photons, the $(\tau)^{-1}$ coefficients refer to spontaneous radiative decay and the Z coefficients to radiationless transfer of energy by inelastic collisions. The primary processes are represented by solid arrows.

$$K(4^2P_{3/2}) + Rb(5^2S_{1/2}) \xrightarrow{Z_{21}'} K(4^2S_{1/2}) + Rb(5^2P_{1/2}) \quad (8)$$

$$K(4^2P_{3/2}) + X(2^2S_{1/2}) \xrightarrow{Z_{21}} K(4^2P_{1/2}) + X(2^2S_{1/2}) \quad (9)$$

$$Rb(5^2P_{3/2}) \xrightarrow{(\tau_{2'})^{-1}} Rb(5^2S_{1/2}) + h\nu_2' \quad (10)$$

$$Rb(5^2P_{1/2}) \xrightarrow{(\tau_{1'})^{-1}} Rb(5^2S_{1/2}) + h\nu_1' \quad (11)$$

$$K(4^2P_{1/2}) \xrightarrow{(\tau_1)^{-1}} K(4^2S_{1/2}) + h\nu_1 \quad (12)$$

$$K(4^2P_{1/2}) + X(2^2S_{1/2}) \xrightarrow{Z_{12}} K(4^2P_{3/2}) + X(2^2S_{1/2}) \quad (13)$$

$$K(4^2P_{1/2}) + Rb(2^2S_{1/2}) \xrightarrow{Z_{12}'} K(4^2S_{1/2}) + Rb(5^2P_{3/2}) \quad (14)$$

$$K(4^2P_{1/2}) + Rb(2^2S_{1/2}) \xrightarrow{Z_{11}'} K(4^2S_{1/2}) + Rb(5^2P_{1/2}) \quad (15)$$

$$Rb(5^2P_{3/2}) + X(2^2S_{1/2}) \xrightarrow{Z_{2'1}'} Rb(5^2P_{1/2}) + X(2^2S_{1/2}) \quad (16)$$

$$Rb(5^2P_{1/2}) + X(2^2S_{1/2}) \xrightarrow{Z_{1'2}'} Rb(5^2P_{3/2}) + X(2^2S_{1/2}) \quad (17)$$

where s_2 is the density of potassium atoms excited per second from the $4^2S_{1/2}$ to the $4^2P_{3/2}$ state, τ_1 and τ_2 are the average lifetimes of the $4^2P_{1/2}$ and $4^2P_{3/2}$ states of potassium respectively, τ_1' and τ_2' are the average lifetimes of the $5^2P_{1/2}$ and $5^2P_{3/2}$ states of rubidium respectively, Z_{12} , Z_{21} , Z_{22}' , Z_{21}' , Z_{12}' , Z_{11}' , $Z_{2'1}'$ and $Z_{1'2}'$ are the frequencies of collisions per excited atom giving rise to radiationless energy transfer, and X represents either a potassium or a rubidium atom in the ground state. Equations (5) - (12) represent the primary processes and equations (13) - (17) represent the secondary reactions.

Some of the secondary processes can be neglected. In the temperature range 80 - 100°C, mixing of the 4^2P states induced by collisions with ground state potassium atoms produces ratios of about 10^{-5} of sensitized-to-resonance fluorescent intensities (Chapman 1965) as does the mixing induced by the more numerous rubidium atoms (Hrycshyn and Krause 1969b). Hence, processes (14) and (15) are negligible in comparison to (7) and (8), respectively, and process (13) is negligible compared with process (5). At rubidium vapour pressures up to 10^{-5} mm Hg, mixing of the 5^2P states also gives ratios of sensitized-to-resonance fluorescent intensities amounting to 10^{-5} , and thus processes (16) and (17) are negligible in comparison with (8) and (10), and (7) and (11), respectively (Rae and Krause 1965). Further simplifications will be introduced at a later stage.

If it is assumed that the K - Rb vapour mixture exists in a steady state which involves only the optical excitation of the potassium $4^2P_{3/2}$ state, spontaneous decay and the various collisional processes shown in Fig. 1, the following rate equations may be written:

$$\frac{dN(4^2P_{3/2})}{dt} = s_2 - N(4^2P_{3/2})[(\tau_2)^{-1} + z_{21} + z_{22} + z_{21}'] = 0 \quad (18)$$

$$\begin{aligned} \frac{dN(4^2P_{1/2})}{dt} = z_{21}N(4^2P_{3/2}) - N(4^2P_{1/2})[(\tau_1)^{-1} + z_{12} + z_{12}' + \\ z_{11}'] = 0 \end{aligned} \quad (19)$$

$$\frac{dN(5^2P_{3/2})}{dt} = z_{22}N(4^2P_{3/2}) - N(5^2P_{3/2})(\tau_2')^{-1} = 0 \quad (20)$$

$$\frac{dN(5^2P_{1/2})}{dt} = z_{21} N(4^2P_{3/2}) - N(5^2P_{1/2}) (\tau_1)^{-1} = 0 \quad (21)$$

where, for example, $N(4^2P_{3/2})$ denotes the density of $4^2P_{3/2}$ potassium atoms and is connected as follows to the observed intensity of fluorescence.

$$I(\nu_2) = \epsilon \frac{h\nu_2}{\tau_2} N(4^2P_{3/2}) \quad (22)$$

ϵ is a measure of the response of the detection system to radiation of frequency ν_2 and is assumed to be the same for all frequencies observed here. Substitution into equations (19), (20), and (21) yields:

$$z_{21} = \frac{\tau_1 \lambda_1}{\tau_2 \lambda_2} [(\tau_1)^{-1} + z_{12} + z_{12}' + z_{11}'] \eta_1 \quad (23)$$

$$z_{22}' = (\tau_2)^{-1} \frac{\lambda_2'}{\lambda_2} \eta_{22}' \quad (24)$$

$$z_{21}' = (\tau_2)^{-1} \frac{\lambda_1'}{\lambda_2} \eta_{21}' \quad (25)$$

where $\lambda_1 = 7699 \text{ \AA}$, $\lambda_2 = 7665 \text{ \AA}$, $\lambda_1' = 7948 \text{ \AA}$ and $\lambda_2' = 7800 \text{ \AA}$. η_1 , η_{22}' , and η_{21}' represent ratios of sensitized-to-resonance fluorescent intensities which are measured experimentally.

$$\eta_1 = \frac{I(7699 \text{ \AA})}{I(7665 \text{ \AA})}, \quad \eta_{22}' = \frac{I(7800 \text{ \AA})}{I(7665 \text{ \AA})}, \quad \eta_{21}' = \frac{I(7948 \text{ \AA})}{I(7665 \text{ \AA})}. \quad (26)$$

If, instead, the potassium $4^2P_{1/2}$ state is optically excited, the following equations result:

$$z_{12} = \frac{\tau_2 \lambda_2}{\tau_1 \lambda_1} [(\tau_2)^{-1} + z_{21} + z_{22}' + z_{21}'] \eta_2 \quad (27)$$

$$z_{12}' = (\tau_1)^{-1} \frac{\lambda_2'}{\lambda_1} \eta_{12}' \quad (28)$$

$$z_{11}' = (\tau_1)^{-1} \frac{\lambda_1'}{\lambda_1} \eta_{11}' \quad (29)$$

where

$$\eta_2 = \frac{I(7665 \text{ \AA})}{I(7699 \text{ \AA})}, \quad \eta_{12}' = \frac{I(7800 \text{ \AA})}{I(7699 \text{ \AA})}, \quad \eta_{11}' = \frac{I(7948 \text{ \AA})}{I(7699 \text{ \AA})}. \quad (30)$$

In all intensity ratios (η -values) defined in equations (26) and (30), the components appearing in the denominators are of the same wavelengths as those used for the excitation of fluorescence.

Since the separation of the potassium resonance doublet is small, setting $\tau_1 = \tau_2 = \tau$ and $\lambda_1 = \lambda_2$ introduces a negligible error in equations (23) and (27). The further conditions that $(z_{12}' + z_{11}') \ll (\tau)^{-1}$ and $(z_{22}' + z_{21}') \ll (\tau)^{-1}$, which were found true over the complete experimental range, simplify the solutions of equations (23) and (27) in the following manner.

$$z_{21} = \frac{1}{\tau} \left(\frac{\eta_1 + \eta_1 \eta_2}{1 - \eta_1 \eta_2} \right) \quad (31)$$

$$z_{12} = \frac{1}{\tau} \left(\frac{\eta_2 + \eta_1 \eta_2}{1 - \eta_1 \eta_2} \right) \quad (32)$$

When η_1 and η_2 are very small (in fact, about 10^{-4}), equations (31) and (32) become further simplified:

$$z_{21} = \frac{\eta_1}{\tau}, \quad z_{12} = \frac{\eta_2}{\tau} \quad (33)$$

Since z_{12} and z_{21} include the combined rates at which the energy of potassium atoms, optically excited to a particular 2P

substate, is transferred to the other substate by collisions with potassium and rubidium atoms in their ground states, they can be represented as follows:

$$\begin{aligned} Z_{12} &= Z'_{12} + Z''_{12} \\ Z_{21} &= Z'_{21} + Z''_{21} \end{aligned} \tag{34}$$

where Z'_{12} and Z'_{21} refer to collisions with potassium and rubidium atoms respectively. Eqs. (34) then become

$$\begin{aligned} Z''_{12} &= \frac{(\eta_2 - \eta'_2)}{\tau} = \frac{\eta''_2}{\tau} \\ Z''_{21} &= \frac{(\eta_1 - \eta'_1)}{\tau} = \frac{\eta''_1}{\tau} \end{aligned} \tag{35}$$

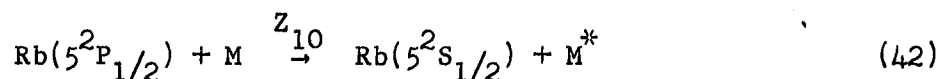
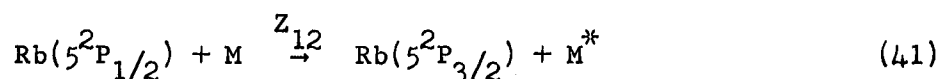
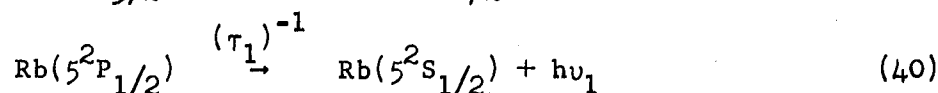
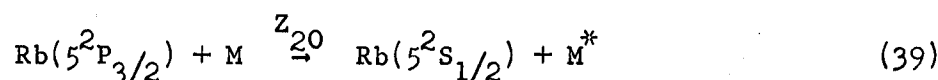
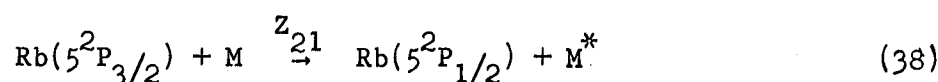
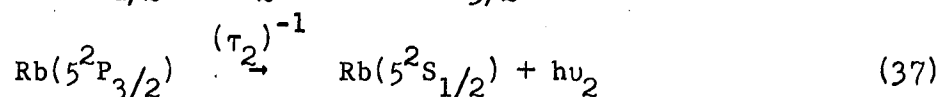
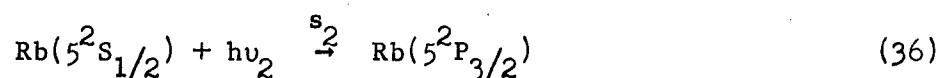
Since the values Z'_{12} and Z'_{21} are known (Chapman and Krause 1965), Z''_{12} and Z''_{21} may be obtained directly.

Equations (24), (25), (28), (29) and (35) connect the total collision cross sections with the experimentally measurable intensity ratios.

B. Collisions Between Excited Rubidium Atoms and Ground State Diatomic or Polyatomic Molecules

Since only one species of alkali atom is involved, the number of collisional mixing processes is considerably smaller than that considered in Section A above. However, while in the previous case the entire transfer of energy by collisions with atoms could be detected as sensitized fluorescence, molecules are capable of quenching excited atoms to their ground states without the emission of

radiation. The mixing and quenching processes that occur when the vapour-gas mixture is optically excited to the rubidium $5^2P_{3/2}$ state are represented in Fig. 2. The various processes are represented by the following equations:



where s_2 is the density of rubidium atoms excited per second from the ground state to the $5^2P_{3/2}$ state, τ_1 and τ_2 are the average lifetimes of the $5^2P_{1/2}$ and $5^2P_{3/2}$ states respectively, Z_{12} , Z_{21} , Z_{10} , Z_{20} are the collision numbers defined as the frequencies of collisions per excited rubidium atom leading to the collision mixing processes $^2P_{1/2} \rightarrow ^2P_{3/2}$, $^2P_{3/2} \rightarrow ^2P_{1/2}$, and the quenching processes $^2P_{1/2} \rightarrow ^2S_{1/2}$ and $^2P_{3/2} \rightarrow ^2S_{1/2}$, respectively, M is a molecule in its ground state and M^* is a molecule whose translational, vibrational and rotational energy has changed as a result of an inelastic collision. The mixing of the 2P substates is assumed to be entirely induced by collision with molecules since the sensitized-to-resonance fluorescent

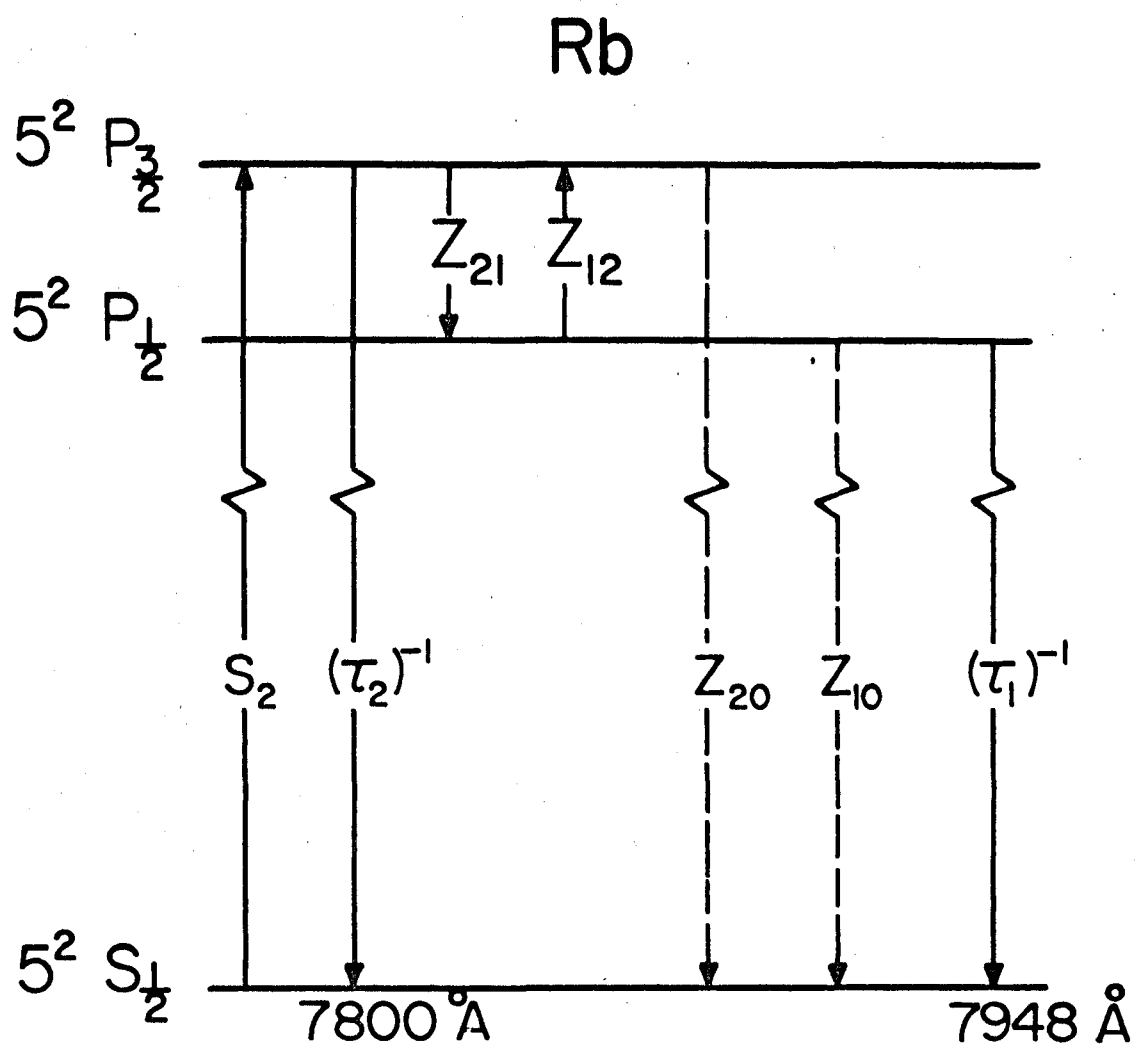


Fig. 2. Energy levels involved in sensitized fluorescence of Rb and in the quenching of the Rb resonance radiation induced by collisions with diatomic and polyatomic molecules.

intensity ratios due to collisions with other rubidium atoms are about 10^{-6} at the vapour pressures used in these experiments (10^{-6} mm Hg) (Rae and Krause 1965); this is at least two orders of magnitude smaller than the values observed at the lowest gas pressures used.

If it is again assumed that the vapour-gas mixture exists in a steady state which involves only the optical excitation of the rubidium $5^2P_{3/2}$ state, spontaneous decay and the collisional processes indicated in Fig. 2, the following rate equations may be written:

$$\begin{aligned} \frac{dN(5^2P_{3/2})}{dt} = s_2 + z_{12}N(5^2P_{1/2}) - N(5^2P_{3/2})[(\tau_2)^{-1} \\ + z_{21} + z_{20}] = 0 \end{aligned} \quad (43)$$

$$\begin{aligned} \frac{dN(5^2P_{1/2})}{dt} = z_{21}N(5^2P_{3/2}) - N(5^2P_{1/2})[(\tau_1)^{-1} + z_{12} \\ + z_{10}] = 0 \end{aligned} \quad (44)$$

where, for example, $N(5^2P_{3/2})$ represents the density of rubidium atoms in the $5^2P_{3/2}$ state. By relating the densities of the excited atoms to the intensities of the resonance components, eq. (44) becomes

$$z_{21} = \frac{\tau_1 \lambda_1}{\tau_2 \lambda_2} [(\tau_1)^{-1} + z_{12} + z_{10}] \eta_1 \quad (45)$$

If the rubidium $5^2P_{1/2}$ state is optically excited instead, the following equation is obtained:

$$z_{12} = \frac{\tau_2 \lambda_2}{\tau_1 \lambda_1} [(\tau_2)^{-1} + z_{21} + z_{20}] \eta_2 \quad (46)$$

where

$$\eta_1 = \frac{I(7948 \text{ \AA})}{I(7800 \text{ \AA})} \quad \text{and} \quad \eta_2 = \frac{I(7800 \text{ \AA})}{I(7948 \text{ \AA})} \quad (47)$$

$\lambda_1 = 7948 \text{ \AA}$ and $\lambda_2 = 7800 \text{ \AA}$. The components appearing in the denominators of eq. (47) are of the same wavelengths as that used for the excitation of fluorescence. Solutions of eqs. (45) and (46) for Z_{12} and Z_{21} lead to the following equations.

$$Z_{21} = A + BZ_{10} + CZ_{20} \quad (48)$$

$$Z_{12} = D + EZ_{20} + CZ_{10} \quad (49)$$

where

$$\begin{aligned} A &= (\tau_2)^{-1} \frac{\eta_1[\lambda_1/\lambda_2 + \eta_2]}{[1 - \eta_1\eta_2]} \\ B &= \tau_1 \frac{(\tau_2)^{-1} \lambda_1/\lambda_2 \eta_1}{[1 - \eta_1\eta_2]} \\ C &= \frac{\eta_1\eta_2}{[1 - \eta_1\eta_2]} \\ D &= (\tau_1)^{-1} \frac{\eta_2[\lambda_2/\lambda_1 + \eta_1]}{[1 - \eta_1\eta_2]} \\ E &= \tau_2 \frac{(\tau_1)^{-1} \lambda_2/\lambda_1 \eta_2}{[1 - \eta_1\eta_2]} \end{aligned} \quad (50)$$

At low gas pressures, quenching effects are negligible and eqs. (48) and (49) reduce to $Z_{21} = A$ and $Z_{12} = D$. If the mixing cross sections are known, the quenching cross sections can be obtained as follows.

Equations (48) and (49) may be rewritten in the form

$$Z_{21} - A = \Delta_{21} = BZ_{10} + CZ_{20} \quad (51)$$

$$Z_{12} - D = \Delta_{12} = EZ_{20} + CZ_{10} \quad (52)$$

Equations (51) and (52) may be solved for Z_{20} and Z_{10} , giving

$$Z_{10} = \frac{\lambda_2 \tau_2}{\lambda_1 \tau_1} \left(\frac{\Delta_{21}}{\eta_1} \right) - \Delta_{12} \quad (53)$$

$$Z_{20} = \frac{\lambda_1 \tau_1}{\lambda_2 \tau_2} \left(\frac{\Delta_{12}}{\eta_2} \right) - \Delta_{21} \quad (54)$$

Once the mixing cross sections have been obtained from the low-pressure data, the collision numbers can be determined at any pressure. The deviations of these collision numbers from the experimentally determined coefficients A and D in eqs. (51) and (52) yield the quantities Δ_{12} and Δ_{21} which are used in eqs. (53) and (54) to determine the collision numbers Z_{10} and Z_{20} , from which the quenching cross sections Q_{10} and Q_{20} may be calculated.

C. Calculation of the Cross Sections

For any collisional process where an atom in state 'a' is transferred to another state 'b', the collision numbers Z_{ab} can, by analogy with the gas kinetic cross section, be related to the average total cross section Q_{ab} ;

$$Z_{ab} = N v_r Q_{ab} \quad (55)$$

where N is the density of ground state atoms or molecules, and v_r is the average relative velocity of the colliding partners, given by

$$v_r = (8kT/\pi\mu)^{1/2} \quad (56)$$

k is the Boltzmann constant, T the absolute temperature and μ the reduced mass. Equation (55) indicates that at a constant temperature, the collision numbers Z_{ab} vary linearly with pressure.

It has been assumed through the discussion in Sections A and B that effects due to radiation trapping are negligible. The imprisonment of radiation, if present, would cause the apparent lifetimes of the resonance states in the alkali atoms to be significantly longer than the 'natural' lifetimes and would manifest itself in the appearance of spuriously large collision cross sections.

The principle of detailed balancing predicts that at a temperature T , the cross sections Q_{12} and Q_{21} should be in the ratio

$$\frac{Q_{12}}{Q_{21}} = \frac{g_2}{g_1} \exp(-\Delta E/kT) \quad (57)$$

where $g_1 = 2$ and $g_2 = 4$ are the statistical weights of the $^2P_{1/2}$ and $^2P_{3/2}$ states, respectively, and ΔE is the energy defect between them. Experimental agreement with the above predicted ratio serves as a good check on the experimental results.

III. DESCRIPTION OF THE APPARATUS

A schematic diagram of the apparatus is shown in Fig. 3. The alkali resonance doublet, emitted by a radio frequency light source, was resolved by a grating monochromator in series with one or two interference filters. The monochromatic beam was then brought to focus in a fluorescence cell which contained the atoms and molecules, the collisions between which were to be studied. The resulting fluorescence, observed at right angles to the direction of the incident beam, was resolved into the two components of the resonance doublet by either three or four interference filters in series, and was focussed on the photocathode of a liquid-air-cooled photomultiplier whose output was registered by one of two methods. The photomultiplier pulses were either integrated and amplified by an electrometer amplifier whose voltage output was fed to a strip chart recorder, or the pulses were counted by a counting train consisting of an amplifier, discriminator and scaler. When employing the pulse-counting method which, on the whole, was preferred, a neutral density filter was inserted into the output beam to attenuate the resonance fluorescence and prevent the scaler from overloading.

A detailed description of the light source has been given elsewhere (Atkinson, Chapman and Krause 1965). The lamp consisted of a tapered pyrex tube which contained about .5 g of distilled alkali metal (either potassium or rubidium) in the tapered end, and

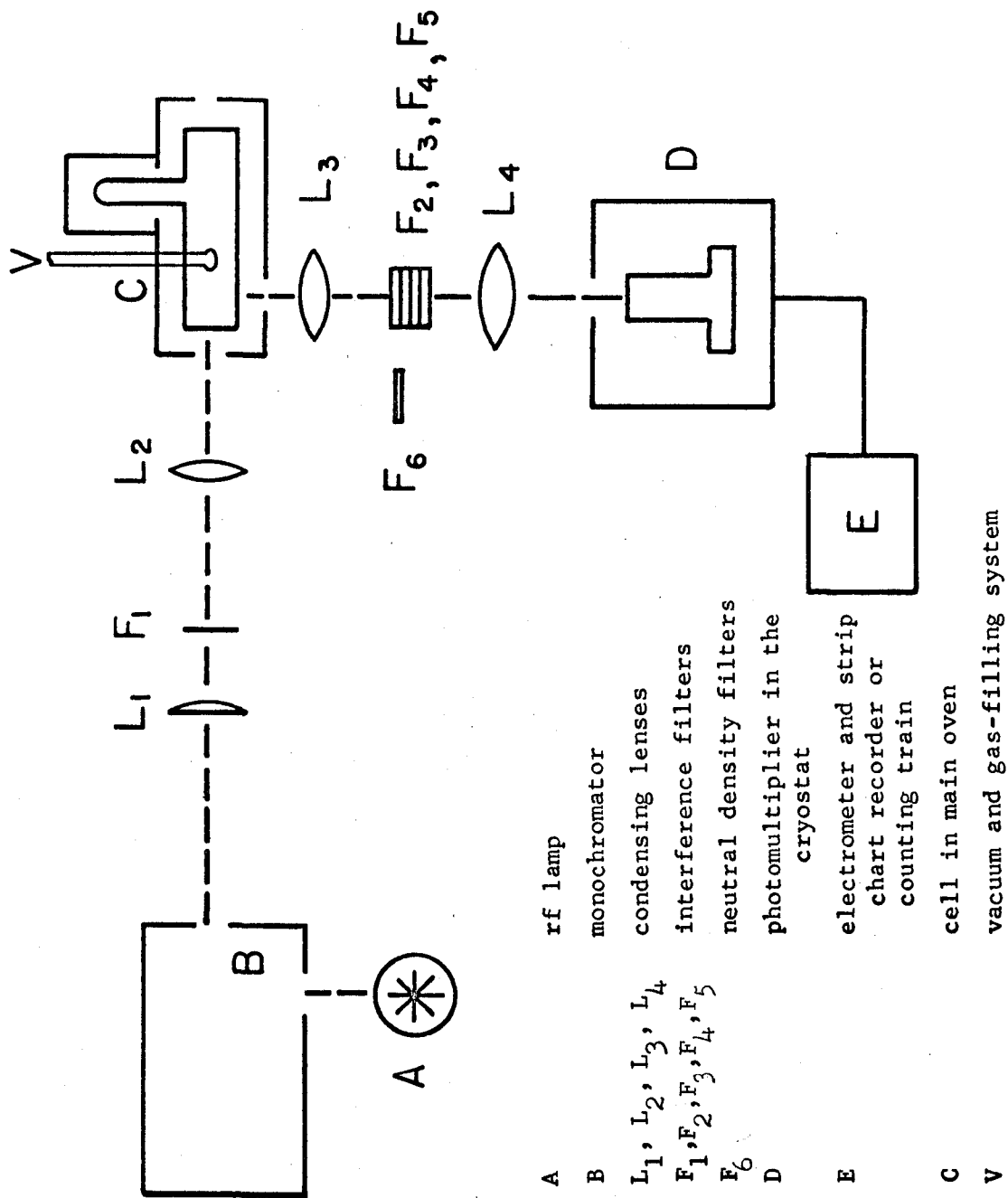


Fig. 3. Schematic arrangement of the apparatus

about 1.5 torr of argon which acted as a carrier gas. The tube was placed in the tank coil of an rf oscillator operating at 60 MHz, with the tapered portion extending down into a wire wound heater coil which was connected through a variac to a voltage-stabilized power line. The temperature of the base of the lamp, which controlled the concentration of alkali vapour, was adjusted until the intensities of the emitted resonance lines were large and stable.

A Bausch and Lomb monochromator was used in conjunction with Spectrolab or Shott interference filters to select one of the potassium or rubidium resonance components from the rf discharge. The monochromator contained a 1200 line/mm grating blazed at 7500 \AA in the first order and had an aperture of $f/4.4$, a focal length of 500 mm and a reciprocal dispersion of 16 \AA/mm in the first order. With the entrance and exit slits set at 1.5 mm wide and 12 mm high, the potassium and rubidium doublets were resolved with a spectral purity of one part in 2,000 and, with the addition of one interference filter, the exciting beam had a spectral purity better than one part in 10^6 . The fluorescent light, however, was resolved only by interference filters. In the observation of sensitized fluorescence in rubidium arising from collisions with excited potassium atoms, four blocked rubidium interference filters were used. Although the rubidium fluorescence was easily resolved (spectral purity of at least one part in 10^{10}), it was found that there was appreciable leakage of potassium resonance radiation through the rubidium filters. Since the transmissions of unwanted lines are difficult to measure in situ, an estimate of the amount of potassium leakage was obtained by

a subsidiary experiment in which a parallel potassium light beam, monochromatic to one part in 10^8 , was passed through the rubidium filters. The transmission of the potassium 7699 Å component through the four rubidium 7800 Å filters mounted in series, which was by far the largest, was measured to be about 10^{-8} . All filter transmissions of the wanted lines were measured in situ.

The design of the fluorescence cell is shown in Fig. 4. Reabsorption of both the exciting light and the fluorescent radiation was minimized by positioning the image of the monochromator slit in the corner formed by the entrance and observation windows. Since a cone of light actually enters the cell, it is not possible to position the image right against the exit window without scattering some of the incident light. The image of the monochromator slit, which was half the size of the actual slit, was centered behind the exit window at a distance of 1.1 mm. With the image in this position, the scattered light, which was further reduced by coating the cell with aquadag (a colloidal dispersion of graphite), was found to be of negligible intensity.

The main oven which contained the body of the cell, consisted of an outer transite box and an inner aluminum box. Chromel A heating wire was wound around the outside of the aluminum box to eliminate glow from the heater, and was insulated from the aluminum by several sheets of asbestos paper. Glass wool, stuffed between the aluminum and transite walls further insulated the oven from the outside. Windows at each end of the oven provided a means of admitting and viewing the incident light and a third window, situated on the

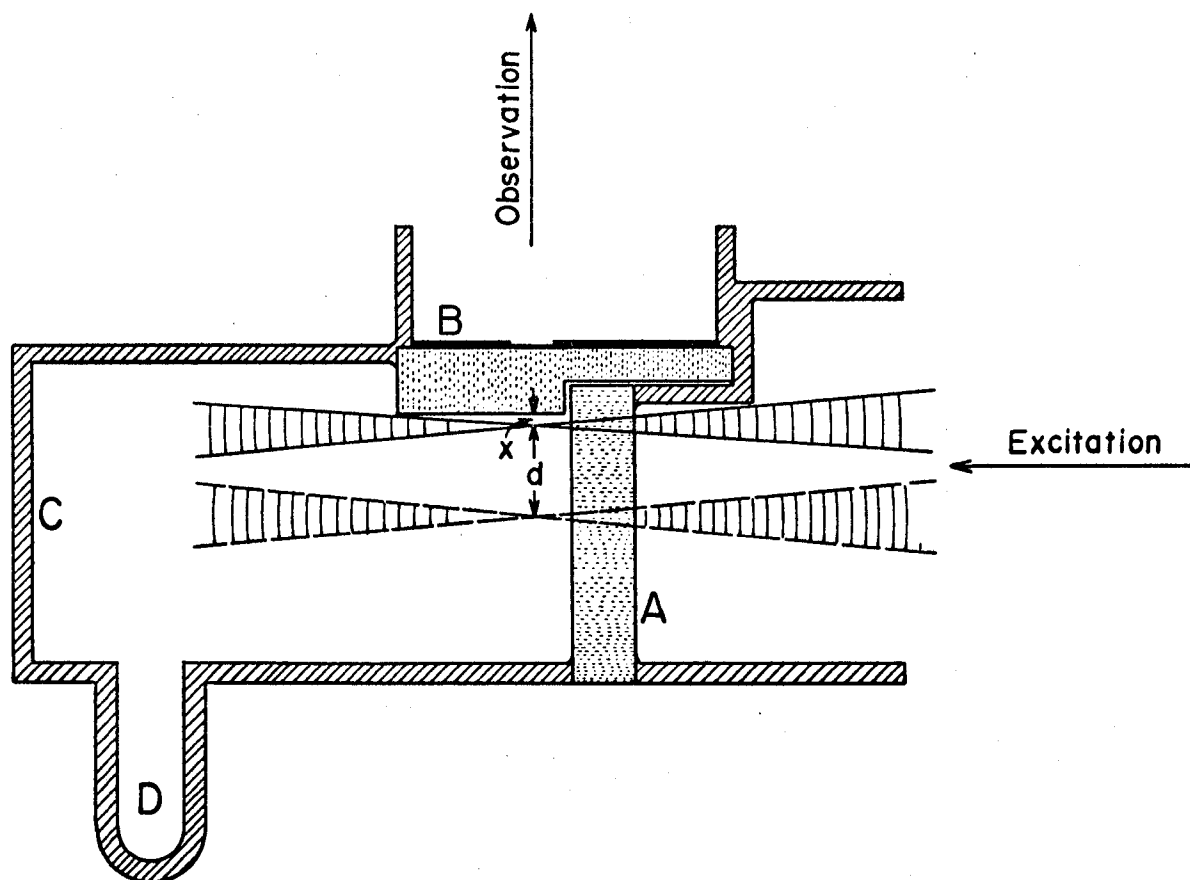


Fig. 4. The fluorescence cell with the ray diagram of the scheme used in the determinations of the extinction coefficients. A, entrance window; B, exit window; C, viewing window; D, side arm.

front wall facing the detection equipment, provided an exit for the fluorescent light. The temperature of the main oven was kept constant to within $\pm 2^{\circ}\text{C}$ by connecting the heater wires through a Variac auto-transformer to a regulated power line.

The side arm of the cell, which was approximately 4 cm long and 12 mm wide, contained the liquid alkali metal. Since the temperature of the side arm determined the vapour density in the main body of the cell (Hoffmann 1962), accurate temperature control was essential. This was accomplished by connecting the side oven, which consisted of a brass cylinder snugly fitting the side arm, to one of two types of temperature controllers. For experiments involving the K - Rb system, where it was necessary to vary the alkali vapour density, resistance wire was wound around the brass cylinder and connected to a thermistor-controlled temperature controller permitting rapid changes in the temperature (Chapman 1965). However, in the study of Rb-molecular gas systems where the side arm temperature was kept constant (40°C), water was circulated from a Jena Ultrathermostat through copper coils mounted in place of the heater wire. In both cases, the temperature was stabilized to within $\pm .2^{\circ}\text{C}$. All temperatures were measured with copper-constantan thermocouples which were located on the main body and on the side arm of the fluorescence cell.

The cell was connected to the vacuum system or gas filling system by a capillary, .23 cm in diameter, which was small enough to prevent migration of the alkali vapour from the cell yet large enough to avoid corrections of the measured gas pressures for molecular transpiration. An Edwards model EO-2 diffusion pump filled with Dow

Corning 704 pumping fluid and backed by a model 1SC50B rotary pump, was used to evacuate the glass system. The system, which also included a liquid air trap, was capable of maintaining a vacuum of better than 10^{-7} torr as measured by a GIC-110B CVC ionization gauge which utilized a GIC-015 gauge head. All molecular gas pressures were first measured approximately by a LKB 3294B autovac gauge and then measured accurately with a CVC McLeod Gauge of type GM-100A connected to a cold trap which was cooled by dry ice immersed in acetone.

The fluorescent light emerging from the cell was focussed on the photocathode of a 16 stage ITT FW-118G photomultiplier tube mounted in a liquid air cryostat. Its S-1 (Ag-O-Cs) photocathode was 3 mm in diameter and had a peak sensitivity around 8000 \AA which differed negligibly for the K and Rb resonance lines. A Fluke 412B power supply supplied 1.8 kilovolts to the resistive divider chain which distributed about 80 volts per dynode of the photomultiplier. The signal from the tube was applied either to a Victoreen VTE-2 electrometer connected to a Philips (PR2216A) strip chart recorder or to a Philips counting train consisting of a preamplifier (PW4270) and scaler (PW4231).

IV. EXPERIMENTAL PROCEDURE

The fluorescence cell was attached to the vacuum system through both the side arm and capillary and was then outgassed for several days at about 150°C at a vacuum of better than 10^{-7} mm Hg. Ampoules containing potassium of 99.95% purity and rubidium of 99.99% purity (supplied by the A. D. McKay Company of New York) were introduced into an extension of the side arm, broken under vacuum and distilled into the side arm which was then sealed off. In preparation of the K - Rb mixture, about .5 g of each metal was distilled into the side arm. The side arm was subsequently heated and cooled until a uniform mixture was formed. In the study of Rb - molecular gas systems, .5 g of rubidium metal was distilled into the side arm. The gases were admitted to the fluorescence cell through the capillary.

The calculations of the various cross sections Q_{ab} for the processes which occur in the K - Rb vapour mixture require an accurate knowledge of the partial pressures of the alkali vapours over the experimental range of temperatures. Specifically, for the processes considered here, the partial pressure of rubidium is required. It has been shown (Rozwadowski and Lipworth 1966) that the usual vapour pressure-temperature formulae for a one-component system are not applicable to a two-component system. This was confirmed by Czajkowski, McGillis and Krause (1966b) who further verified Seiwert's (1956) contention that the partial pressure of one component in the

saturated vapour mixture depended on the composition of the mixture and could be represented by the expression

$$P_1 = \gamma_1 P_0 \quad (58)$$

where P_1 is the partial pressure of one alkali metal in the mixture, P_0 is the vapour pressure of the pure metal at the same temperature and γ_1 is its mole fraction (ratio of the number of gram-atoms of the metal to the total number of gram-atoms present in the mixture). This is effectively a restatement of Raoult's Law. In the present case, the mole fraction may be defined as

$$\gamma_1 = \frac{n(\text{Rb})}{n(\text{Rb}) + n(\text{K})} \quad (59)$$

where $n(\text{Rb})$ and $n(\text{K})$ are the numbers of gram-atoms of rubidium and potassium in the mixture, respectively.

The partial pressure of rubidium vapour in the K - Rb vapour mixture was determined by a method shown to be valid by Czajkowski, McGillis and Krause (1966b), in which the extinction coefficients β were measured over a range of temperatures for the rubidium 7948 \AA resonance component both in vapours of pure rubidium and in the K - Rb vapour mixture. This method is depicted in Fig. 4 which shows the incident beam passing through the cell. The image of the monochromator slit, which was reduced to a width of .05 mm, was moved back and forth along the axis of observation by displacing the lens L_2 in Fig. 3 through a distance $d = 1 \text{ mm}$ by means of a micrometric device precisely calibrated using a cathetometer. The extinction coefficient β was calculated from the expression:

$$\beta = \frac{\ln I_0 - \ln I}{d} \quad (60)$$

where I_0 and I are the fluorescent intensities corresponding to $d = 0$ and $d = 1$ mm, respectively. From plots of the extinction coefficients against temperature for both pure rubidium and rubidium in the K - Rb mixture, γ_1 was obtained so that equation (58) could be used to determine the partial pressures of rubidium vapour. The vapour pressure of pure rubidium was taken from temperature-vapour pressure data given by Nesmeyanov (1963). Although in the calculations of the collision cross sections for the processes occurring in the Rb-molecular gas systems, an exact knowledge of the rubidium vapour density is not required; however, the vapour density must be kept low to avoid imprisonment of radiation. This was achieved by maintaining the side arm at 40°C , which corresponds to a rubidium vapour density much lower than that at which radiation imprisonment becomes appreciable for this type of geometry (Rae and Krause 1965).

The following gases were used: H_2 (99.9995% purity), N_2 (99.999%), CH_4 (99.99%), C_2H_4 (99.98%), C_2H_6 (99.9%), D_2 (>99.5% isotopic purity), all supplied by Matheson of Canada, Ltd., Whitby, Ontario, and HD ($\geq 98.38\%$ isotopic purity) and CD_4 ($\leq 96.97\%$) supplied by Merck, Sharp and Dohme of Canada, Ltd., Montreal, Quebec. Chemically active impurities were removed from the gases by allowing them to remain for a few days in a rubidium-coated glass bulb which was heated to about 100°C . Before being admitted into the fluorescence cell, the gases were passed through a liquid-air cooled trap to remove any rubidium vapour carried by the gas.

The McLeod gauge gas pressure measurements were not corrected for molecular transpiration which occurs in the capillary connecting the fluorescence cell to the rest of the gas system when the mean free paths of the gas molecules are larger than the diameter of the capillary (Dushman and Lafferty 1962) since only those points taken at very low gas pressures (usually below 0.05 mm Hg) are affected. Also, over the range of experimental pressures used, errors arising from the streaming of mercury vapour towards the cold trap could be neglected (Bennewitz and Dohmann 1965).

V. SENSITIZED FLUORESCENCE IN K - Rb VAPOUR MIXTURES

A. The Extinction Coefficients

Plots of the extinction coefficients for the 7948 Å rubidium component against temperature for both pure rubidium and for the K - Rb mixture are shown in Fig. 5. (All the experimental values of the extinction coefficients are listed in Appendix A.) Because the extinction coefficients are functions of the density of the rubidium atoms in the vapour, therefore for any specific temperature of the mixture the corresponding temperature (and hence the vapour pressure) of pure rubidium can be read off the plots. In this way it was possible to determine the partial pressures of the rubidium in the K - Rb mixture. The ratio of the partial pressure of rubidium in the mixture at a particular temperature to the vapour pressure of pure rubidium at the same temperature yielded γ_1 , the mole fraction of rubidium in the mixture. It was found that, over the temperature range shown in Fig. 5, $\gamma_1 = 0.37 \pm 0.01$, where 0.01 is the mean deviation. Substitution of this value in equation (58) yielded $P_1 = 0.37 P_0$, which was used to determine the partial pressure of the rubidium vapour.

The extinction coefficients of the mixture were also measured for the 7800 Å rubidium component as well as for both components of the potassium resonance doublet. On the basis of these measurements, eq. (60) was utilized to correct for the attenuation

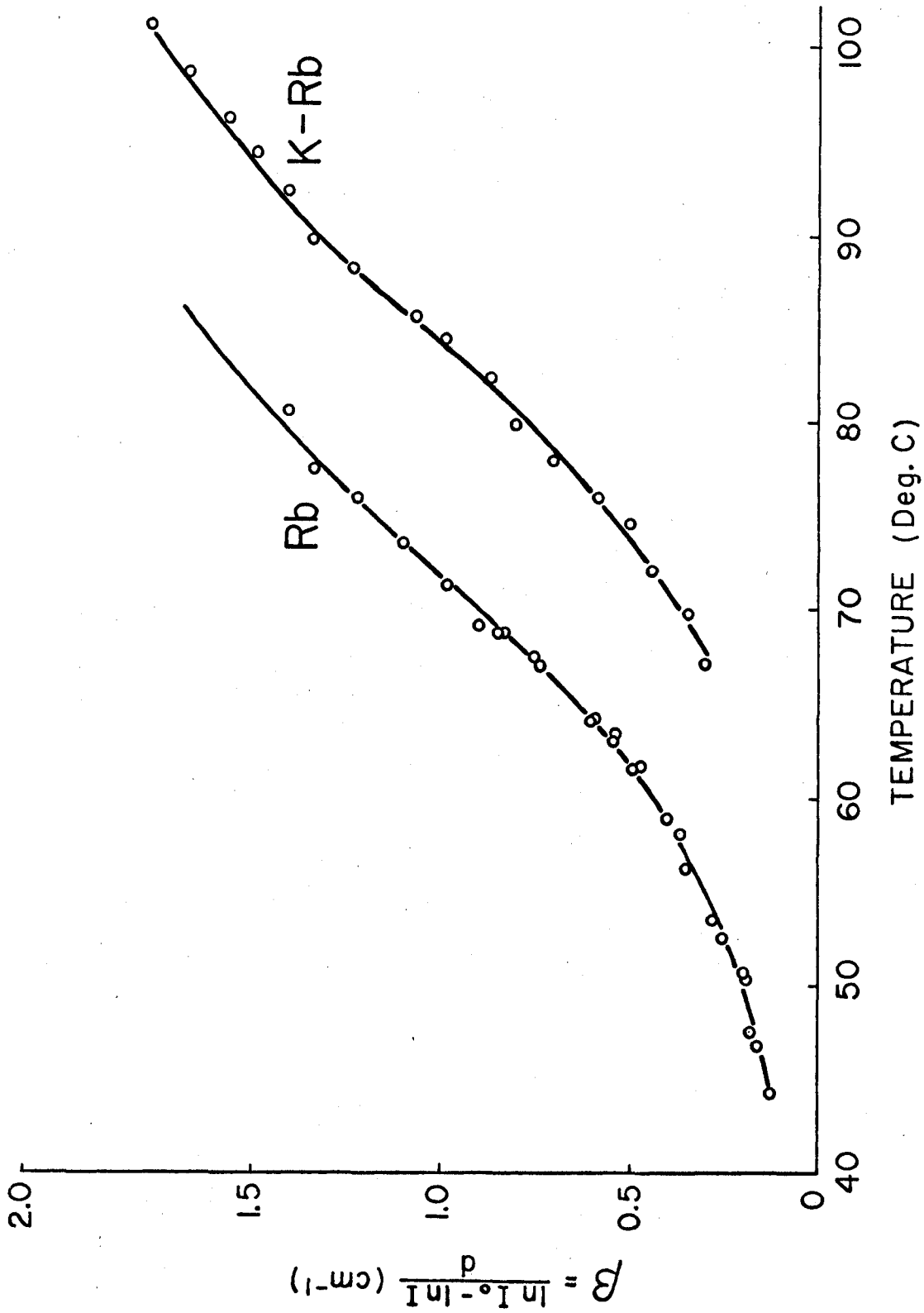


Fig. 5. The variation with temperature of the extinction coefficients for the 7948 Å component in pure rubidium vapour and in the potassium-rubidium vapour mixture.

of the fluorescent intensities which was due to reabsorption of the fluorescence as it traversed the distance of 1.1 mm in the vapour. These corrections to the observed intensity ratios amounted to as much as 17% when the 7800 Å component was observed in sensitized fluorescence, and to at most 10% for the 7948 Å component. When either the 7665 Å or the 7699 Å component was observed in sensitized fluorescence, the intensity ratios were adjusted by a maximum of 3%.

B. The Cross Sections for K - Rb Collisions

(i) Energy Transfer from the 2P Substates of Potassium to the 2P Substates of Rubidium, Induced in Collisions with Ground State Rubidium Atoms

Plots of the intensity ratios* η_{12} , η_{22} , η_{11} , and η_{21} , against rubidium vapour pressure are shown in Figs. 6, 7, 8 and 9, respectively. As has been observed previously in similar experiments Czajkowski, McGillis and Krause (1966b), the curves depart from linearity because of changes in the lifetimes of the potassium 4^2P states [which were assumed constant in equations (24), (25), (28) and (29)], caused by the imprisonment of the potassium resonance radiation which sets in with increasing density of potassium atoms. In Figs. 6 and 7, the linear portions are well-defined and thus the cross sections Q_{12} , and Q_{22} , can be calculated by the direct applications of equations (24), (28) and (55). In Figs. 8 and 9, however, the low intensity of sensitized fluorescence made possible the measurement

* The numerical data is listed in Appendix A.

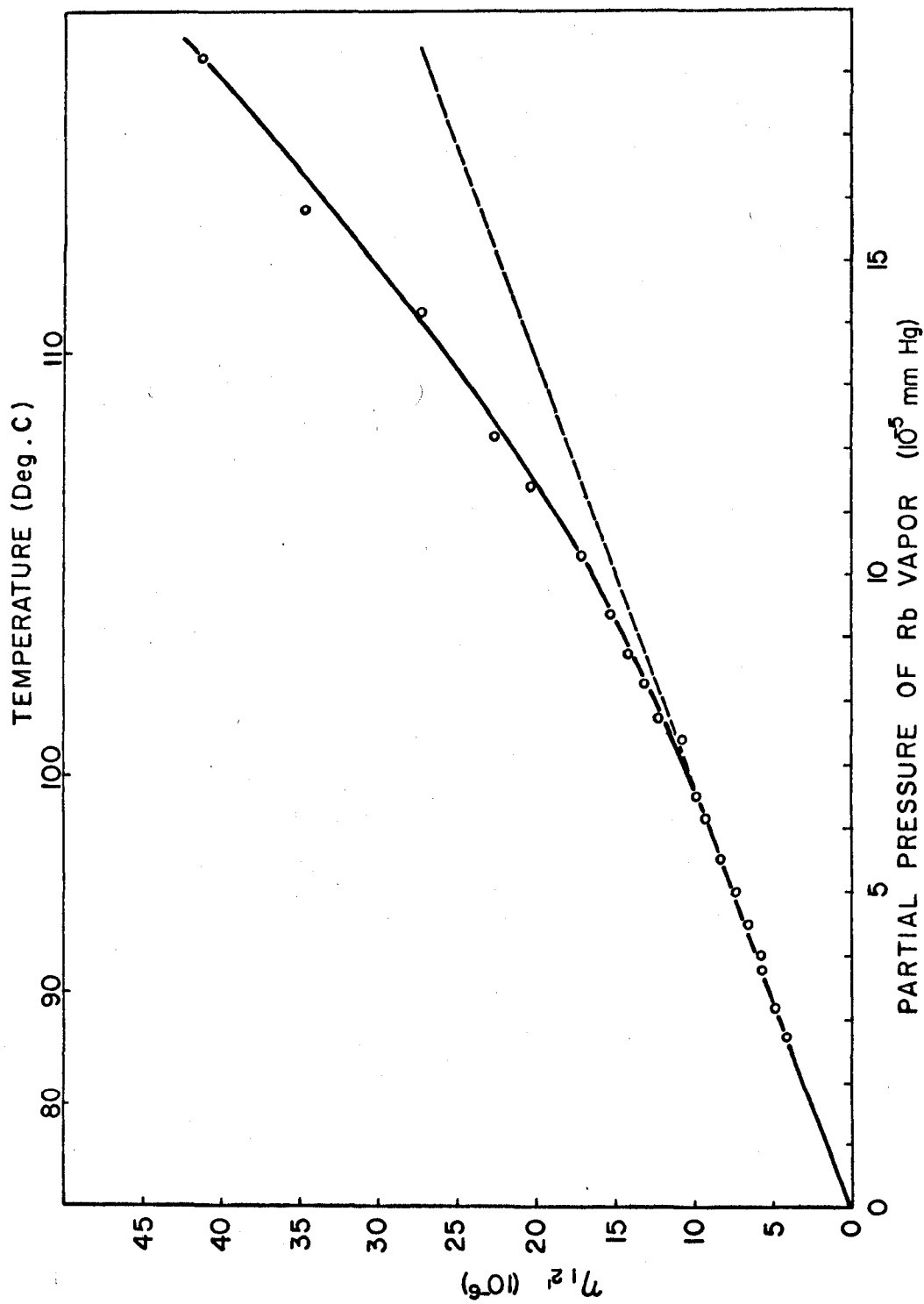


Fig. 6. A plot of the intensity ratio η_{12} , against temperature. The statistical errors are negligible.

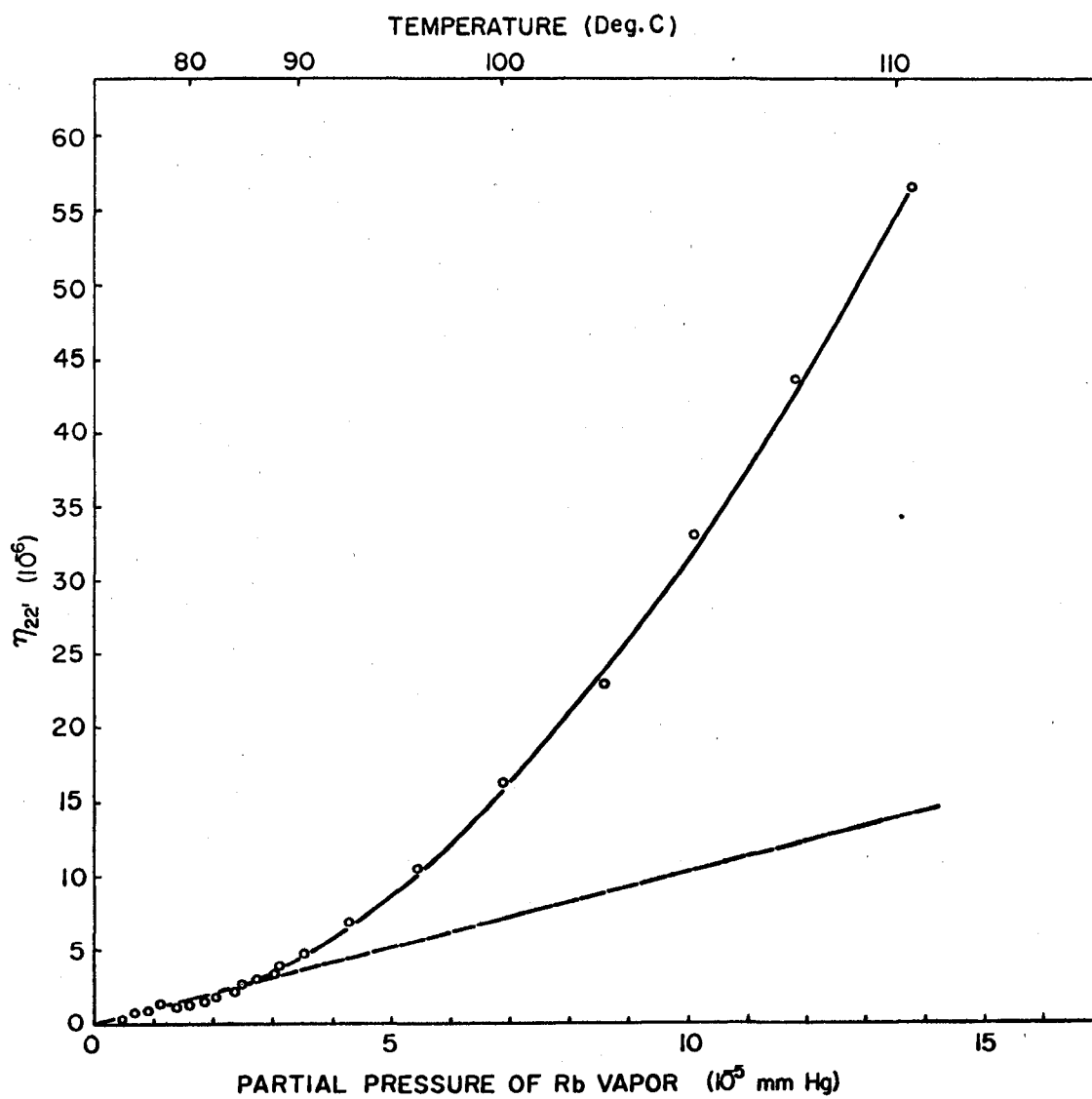


Fig. 7. A plot of the intensity ratio η_{22}' against temperature. The statistical errors are negligible.

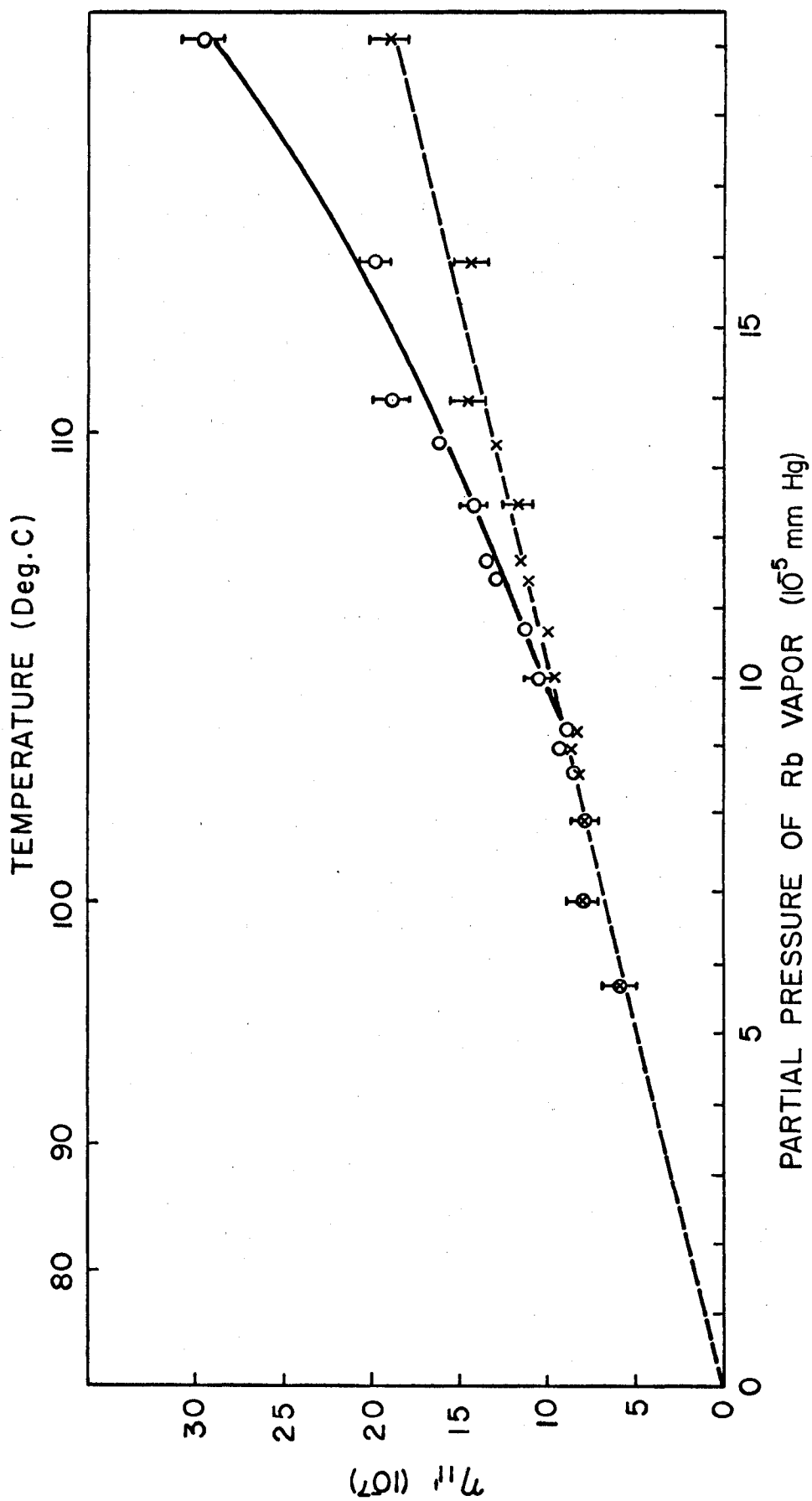


Fig. 8. A plot of the intensity ratio η_{11} , against temperature. (o) experimental results; (x) results corrected for reabsorption and trapping of resonance radiation. The error bars represent typical errors derived from counting statistics.

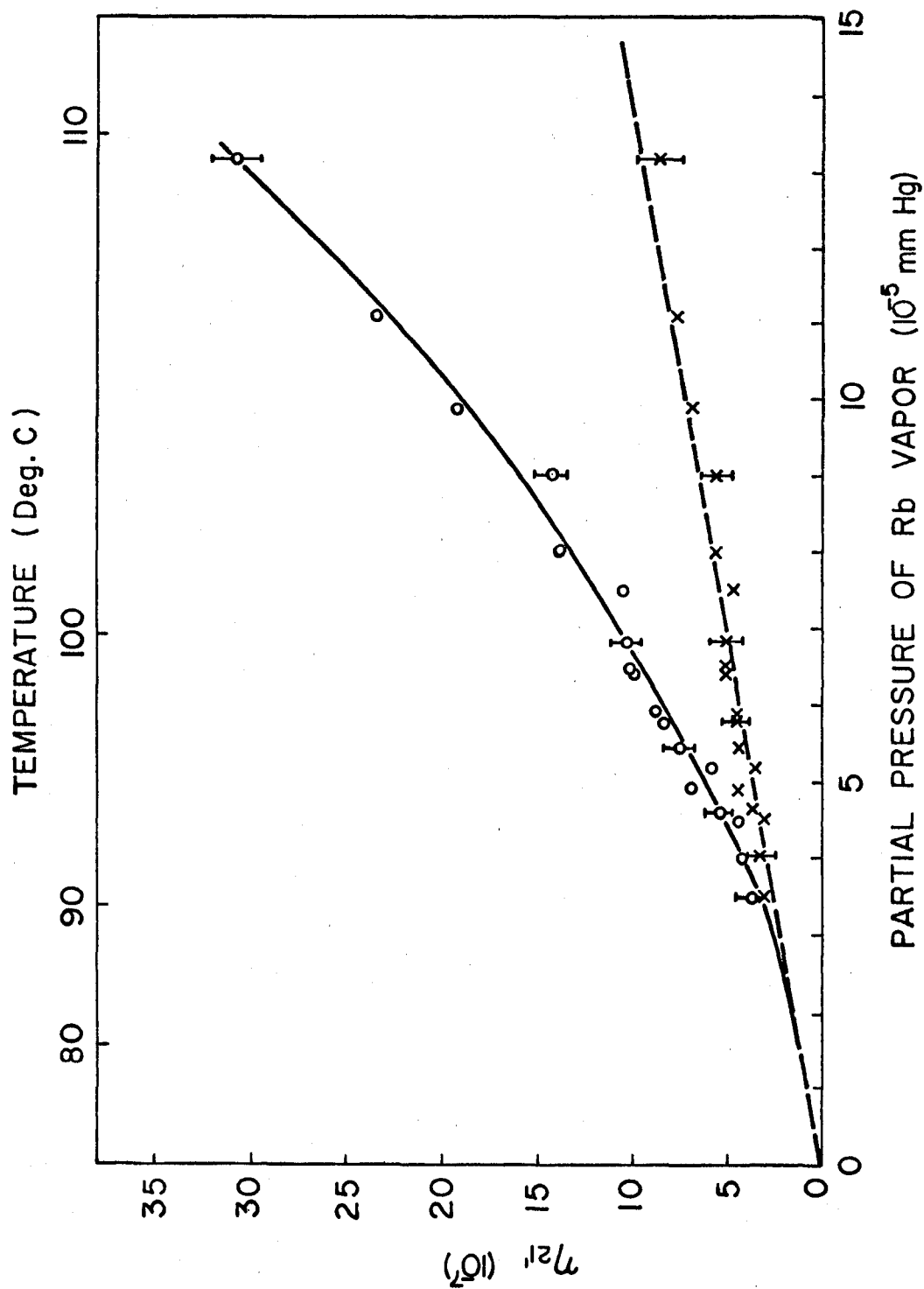


Fig. 9. A plot of the intensity ratio η_{21} against temperature. (o) experimental results; (x) results corrected for reabsorption and trapping of resonance radiation. The error bars represent typical errors derived from counting statistics.

of η -values only at pressures where radiation imprisonment was already becoming significant. The following procedure was used to correct these curves for radiation trapping.

In the case of Fig. 6, the appropriate cross section can be written:

$$Q_{12}' = \frac{\eta_{12}'}{\tau_1 N v_r} \quad (61)$$

where η_{12}' represents the values lying on the linear portion including the extrapolated region indicated by the dashed line. For the points lying on the curved portion, where the effects of radiation trapping are not negligible, the cross section may be written:

$$Q_{12}' = \frac{\eta_{12}'^*}{\tau_1(\text{eff}) N v_r} \quad (62)$$

where the $\eta_{12}'^*$ are the intensity ratios measured in the region of radiation imprisonment and $\tau_1(\text{eff})$ is the effective lifetime of the potassium $4^2P_{1/2}$ state at a particular side arm temperature (Hoffmann and Seiwert 1961). Because equations (61) and (62) are assumed to give the same cross section Q_{12}' , therefore, for any given temperature

$$\frac{\eta_{12}'^*}{\eta_{12}'} = \frac{\tau_1(\text{eff})}{\tau_1} \quad (63)$$

Similarly, for the case shown in Fig. 8 where the same resonance component (7699 Å) is used for excitation, it follows that

$$\frac{\eta_{11}'^*}{\eta_{11}'} = \frac{\tau_1(\text{eff})}{\tau_1} \quad (64)$$

In this way, $\tau_1(\text{eff})$ at a particular temperature may be obtained from

eq. (63) since $\eta_{12}'^*$, η_{12}' , and τ_1 are known. Substitution into eq. (64) gives η_{11}' , the corrected η value.

Since the linear portion in Fig. 7 is also well-defined, it follows that the expression

$$\frac{\eta_{22}'^*}{\eta_{22}'} = \frac{\tau_2(\text{eff})}{\tau_2} \quad (65)$$

can be solved for $\tau_2(\text{eff})$ at any particular temperature thus yielding η_{21}' , the corrected η values in Fig. 9.

In both cases, point-by-point calculations yielded the corrected η values shown in Figs. 8 and 9. In Fig. 8, no corrections were necessary for the lower points which were obtained at vapour densities where radiation imprisonment is virtually absent. The agreement between the results obtained at low pressures and those yielded by the above treatment attests to the validity of the method. It should be noted that in Fig. 7 where the 7665 Å component is used for excitation, nonlinearity of the η -P curve sets in at a potassium partial pressure of approximately 0.55×10^{-5} mm Hg whereas when the 7699 Å component is used for excitation (Fig. 6), the curve becomes non-linear at about 1.20×10^{-5} mm Hg. As expected, the pressures at which nonlinearity sets in are approximately in the reciprocal ratio of the respective oscillator strengths of the two resonance components.

The total cross sections Q_{12}' , Q_{22}' , Q_{11}' , and Q_{21}' , were calculated from the slopes of the linear portions of the graphs in Figs. 6, 7, 8 and 9, respectively, using $\tau_1 = \tau_2 = 2.77 \times 10^{-8}$ s

(Copley and Krause 1969). The results are shown in Table 1 together with the cross sections quoted by other authors.

(ii) Mixing of the 2P Substates of Potassium Induced in Collisions with Ground State Rubidium Atoms

Plots of the intensity ratios* η_1 , η_2 , η_1'' and η_2'' against rubidium vapour pressure are shown in Fig. 10. As before, the plots of η'' are linear at temperatures corresponding to potassium vapour pressures lower than 10^{-5} mm Hg and depart from linearity at higher pressures where the imprisonment of potassium radiation becomes appreciable. The slopes of the η'' curves, used in conjunction with eqs. (35) and (55), yielded the mixing cross sections Q_{12}'' and Q_{21}'' which are quoted in Table 1. The experimental ratio Q_{12}''/Q_{21}'' was found to be 1.5 ± 0.2 which is in satisfactory agreement with the value of 1.60 calculated from eq. (57) at the main oven temperature $T = 370^\circ\text{K}$.

C. Discussion of the K - Rb Cross Sections

The errors quoted in Table 1 were obtained mainly from calculations of the statistical uncertainties arising from counting statistics as well as from estimates of the somewhat larger systematic error inherent in the determination of the partial pressures of rubidium vapour. Although systematic errors are generally difficult to determine, it was estimated that during the course of the experiments, the mole fraction of the rubidium in the K - Rb mixture did not deviate by more than 15%. Filter transmissions for the wanted lines,

* The numerical data is listed in Appendix A.

TABLE 1

Cross Sections for Inelastic Collisions Between
Excited Potassium and Ground State Rubidium Atoms

Designation	Value (\AA) ²	Source
$Q_{12}, (4^2P_{1/2} \rightarrow 5^2P_{3/2})$	40 ± 8	This Investigation
	5.3 ± 0.8	Stacey and Zare (1970)
	10	Dashevskaya et al (1970) (Theor.)
$Q_{22}, (4^2P_{3/2} \rightarrow 5^2P_{3/2})$	27 ± 7	This Investigation
	5.5 ± 1.2	Stacey and Zare (1970)
$Q_{11}, (4^2P_{1/2} \rightarrow 5^2P_{1/2})$	2.7 ± 0.6	This Investigation
	2.2 ± 0.5	Ornstein and Zare (1969)
	4	Dashevskaya et al (1970) (Theor.)
$Q_{21}, (4^2P_{3/2} \rightarrow 5^2P_{1/2})$	1.9 ± 0.6	This Investigation
	2.6 ± 0.5	Ornstein and Zare (1969)
$Q_{12}^{''}, (4^2P_{1/2} \rightarrow 4^2P_{3/2})$	260 ± 65	This Investigation
	<67	Dashevskaya et al (1970) (Theor.)
$Q_{21}^{''}, (4^2P_{1/2} \rightarrow 4^2P_{3/2})$	175 ± 50	This Investigation

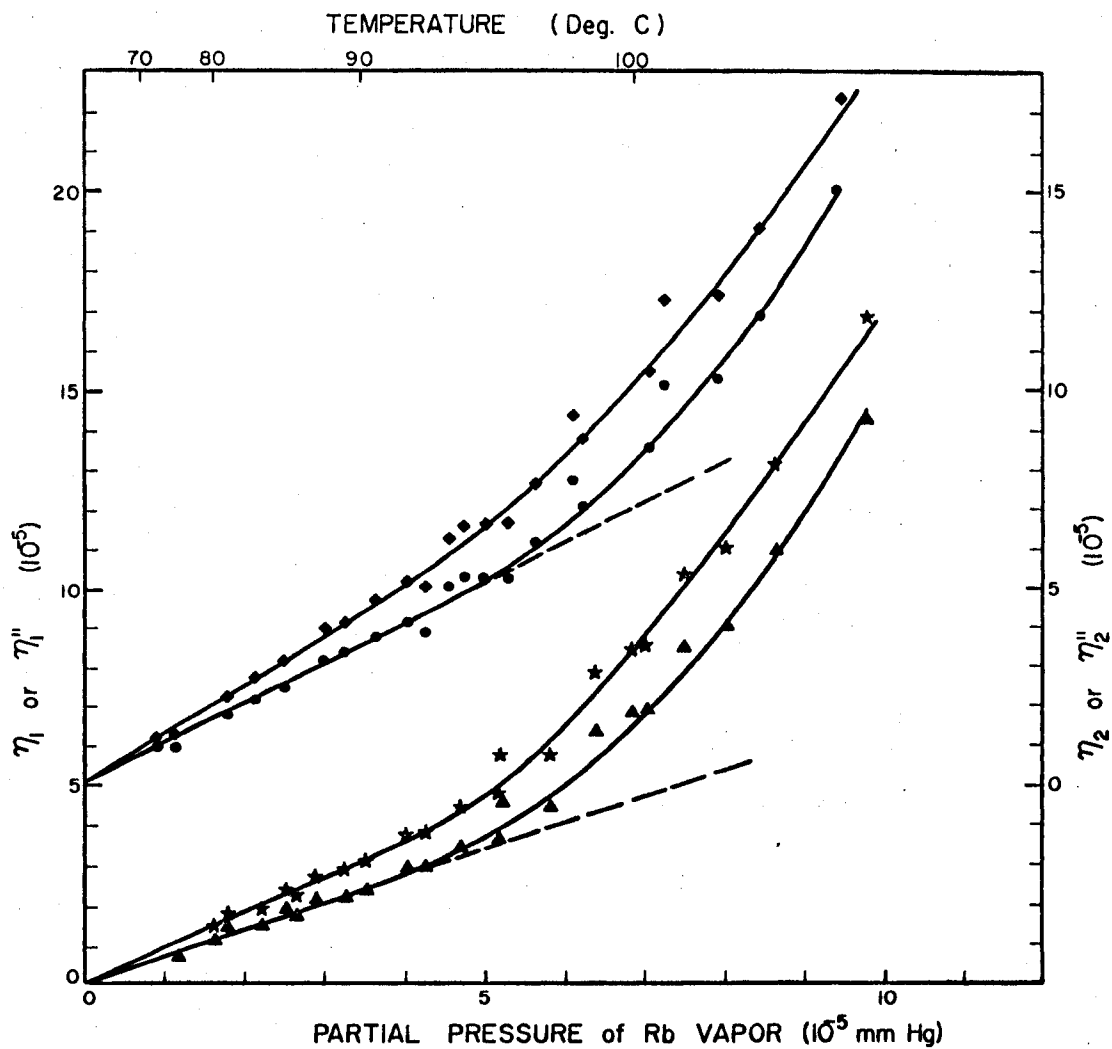


Fig. 10. Plots of intensity ratios η and η' against partial pressure of rubidium vapour. (*) η_1 ; (Δ) η_1' ; (\diamond) η_2 ; (\circ) η_2' . The errors arising from counting statistics are too small to be shown.

which were measured before and after each experimental run were found to be constant within 2% and the lifetimes of the potassium resonance states were accurate to 3% (Copley and Krause 1969). An additional error in the cross sections for the mixing of the potassium 2P states induced in collisions with ground state rubidium atoms, arose because of the uncertainties in the cross sections obtained by Chapman and Krause (1965) for 2P mixing in potassium by collisions between unexcited and excited potassium atoms. This added a 3% uncertainty to the cross section Q'_{12} and 7% to Q'_{21} .

Table 1 shows that the values of the cross sections Q_{11} , and Q_{21} , obtained in this investigation, agree within experimental error with those determined independently by Ornstein and Zare (1969) who used an entirely different technique for the measurement of the partial pressure of rubidium vapour. The fact that different fluorescence cells were used in the two determinations suggests that any anisotropy of the sensitized fluorescence of rubidium, which might occur when the rubidium radiation is trapped, could not have had a serious effect on the results. The values quoted by Stacey and Zare (1970) for the cross sections Q_{12} , and Q_{22} , do not agree with the values determined in this laboratory. Discussions with the authors have thus far not yielded a satisfactory explanation for the discrepancy. Both experiments encountered difficulties with leakage of the potassium fluorescence through the rubidium 7800 Å filters. Stacey and Zare (1970) circumvented this difficulty by using a potassium absorption cell in series with two or three rubidium interference filters to filter out the potassium radiation whereas in this

experiment, four blocked rubidium interference filters resolved the sensitized fluorescence. Although potassium leakage increases the values of the observed intensity ratios, it does not alter the slopes of the η -P plots from which the cross sections were obtained, but appears as a positive intercept. All such intercepts were subtracted from the observed intensity ratios to give the actual η values.

A value of 3.2 \AA^2 obtained by Thangaraj (1948) for the overall cross section for excitation transfer from the 4^2P resonance state of potassium to the 5^2P state in rubidium, is not listed in Table 1 since a meaningful comparison with any particular value found in this investigation is not possible. Thangaraj worked at vapour pressures in the neighbourhood of 0.1 mm Hg where the exciting light is completely absorbed by the surface layer of atoms in the fluorescence cell. Under these conditions, the secondary collisional processes which were deemed negligible here might assume a much greater importance.

Table 1 also compares the experimental results with the theoretical values calculated by Dashevskaya et al (1970) who showed that a dipole-dipole interaction which is responsible for collisional excitation transfer between identical alkali atoms is not sufficient to explain the magnitudes of the cross sections observed in collisions with dissimilar alkali partners. The authors suggest that exchange interactions which come into play as the interatomic distance between colliding partners decreases, must be taken into account. This theory represents a distinct advance over previous attempts in predicting similar experimental cross sections. It should be mentioned that the

discrepancy between the experimental and theoretical values for the cross section $Q_{12}'(4^2P_{1/2} \rightarrow 4^2P_{3/2})$ is of the same order of magnitude as the discrepancy between the experimental and theoretical cross sections for the analogous process induced in collisions between identical partners, such as K - K, Rb - Rb and Cs - Cs (Dashevskaya, Voronin and Nikitin 1969).

VI. SENSITIZED FLUORESCENCE AND QUENCHING INDUCED IN
COLLISIONS OF RUBIDIUM ATOMS WITH MOLECULES

A. The Experimental Results

The experimentally determined intensity ratios η_1 and η_2 are plotted against the pressures of various gases in Figs. 11, 12, 13 and 14. (The numerical data is presented in Appendix B.) Fig. 12 shows the intensity ratios for H_2 , HD and D_2 obtained at low pressures at which quenching effects are negligible and where the collision numbers Z_{12} and Z_{21} can be obtained directly from eqs. (51) and (52) by calculation of the terms D and A, respectively, using $\tau_1 = 2.81 \times 10^{-8}$ s and $\tau_2 = 2.70 \times 10^{-8}$ s (Link 1966). D and A are plotted against HD pressure in Fig. 15 which is representative of all the cases where the mixing cross sections are much larger than the quenching cross sections. It may be seen that at low pressures $Z_{12} = D$ and $Z_{21} = A$ and thus the mixing cross sections can be obtained from the slopes of the Z-P plots used in conjunction with eq. (55). At higher pressures, the differences $\Delta_{21} = Z_{21} - A$ and $\Delta_{12} = Z_{12} - D$ at each experimental point were substituted into eqs. (53) and (54), yielding the collision numbers Z_{10} and Z_{20} . The resulting plots of Z_{10} and Z_{20} against HD pressure are linear and their slopes, as before, gave the corresponding cross sections Q_{10} and Q_{20} .

In the case of the saturated hydrocarbons CH_4 , CD_4 and C_2H_6 , plots of A and D against gas pressures show negligible departures

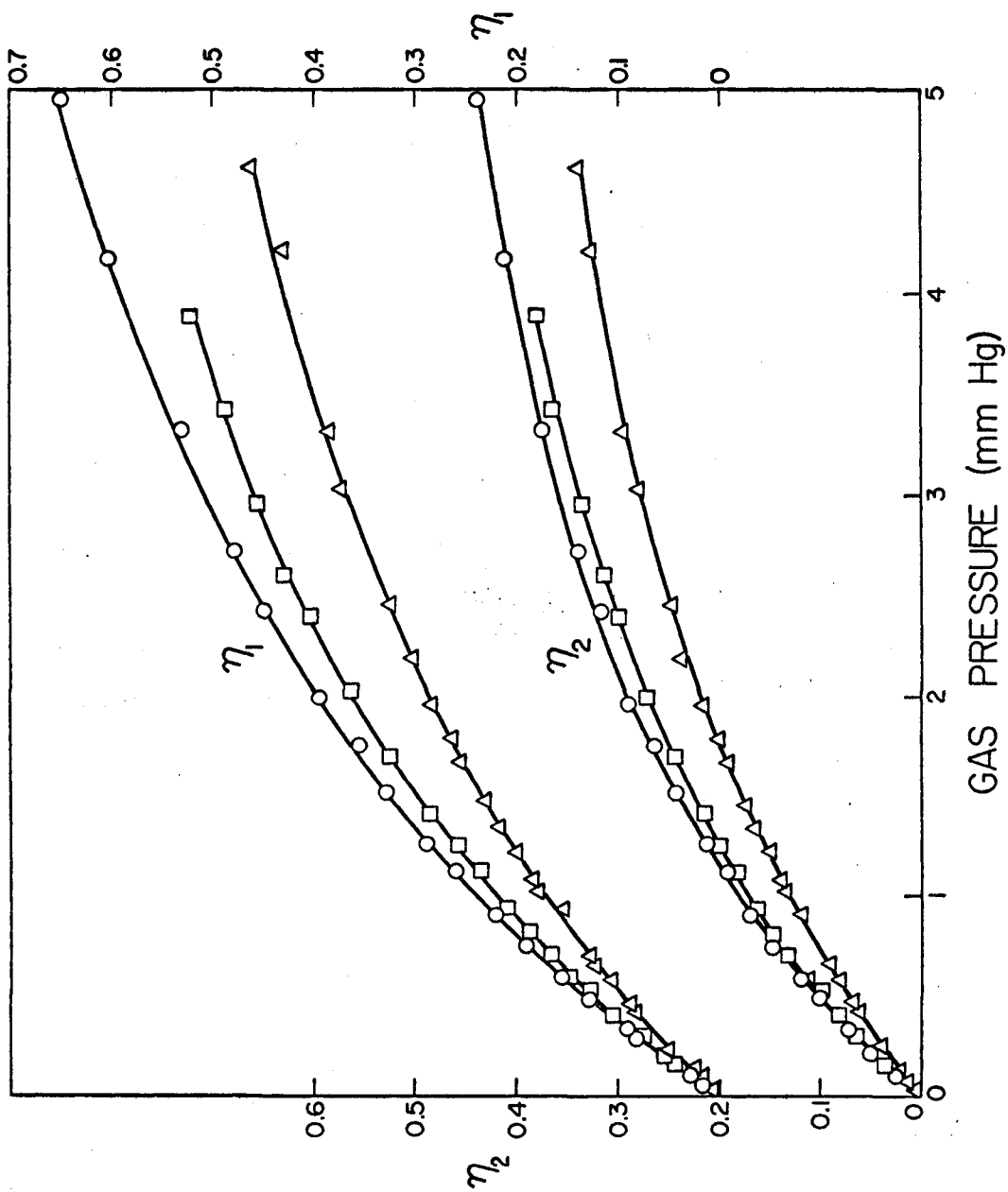


Fig. 11. Plots of intensity ratios η_1 and η_2 against H_2 , HD and D_2 gas pressures. (o) D_2 ; (□) HD; (Δ) H_2 .

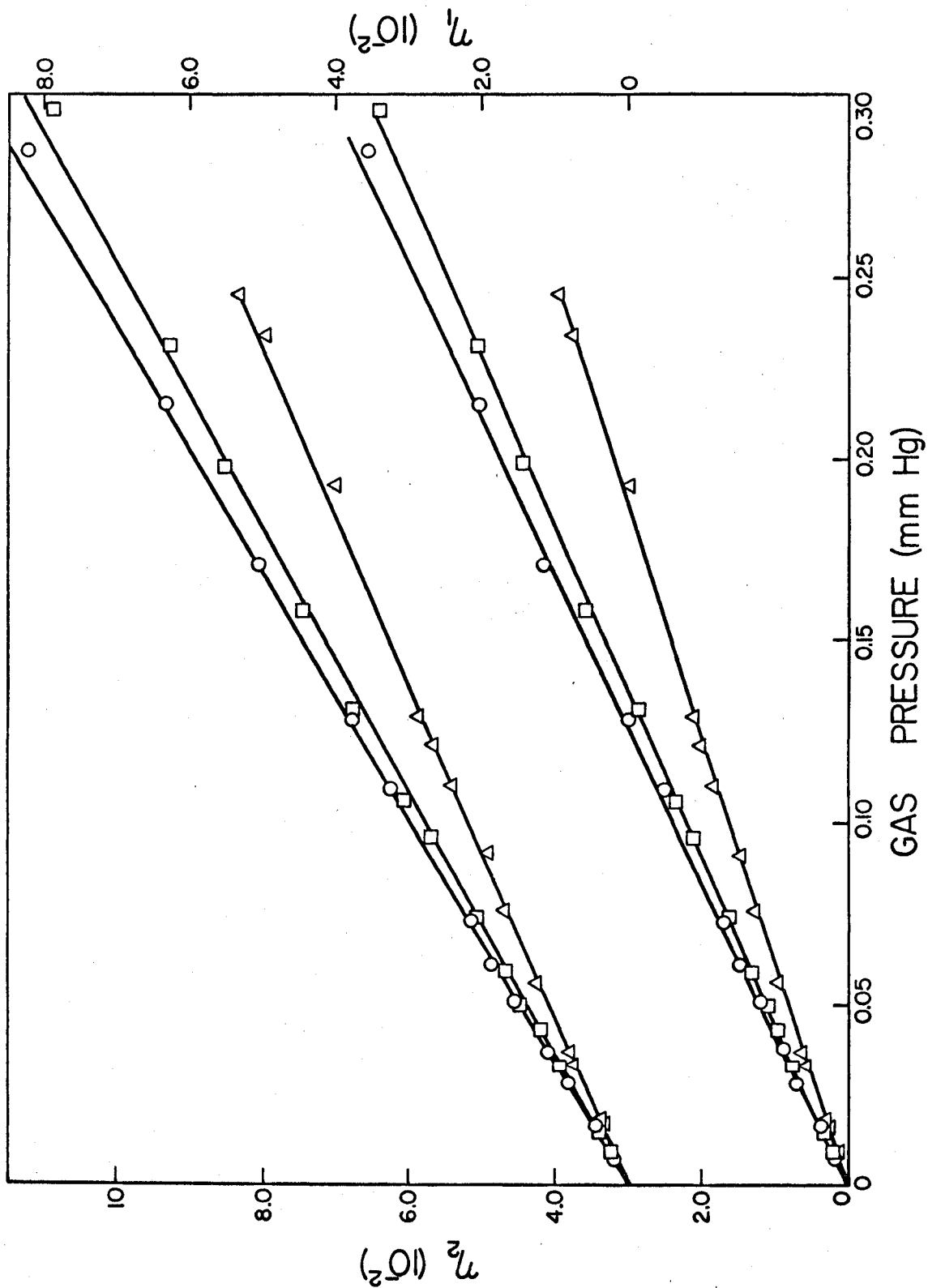


Fig. 12. Plots of intensity ratios η_1 and η_2 against H_2 , HD and D_2 gas pressures. (o) D_2 ; (\square) HD; (Δ) H_2 .

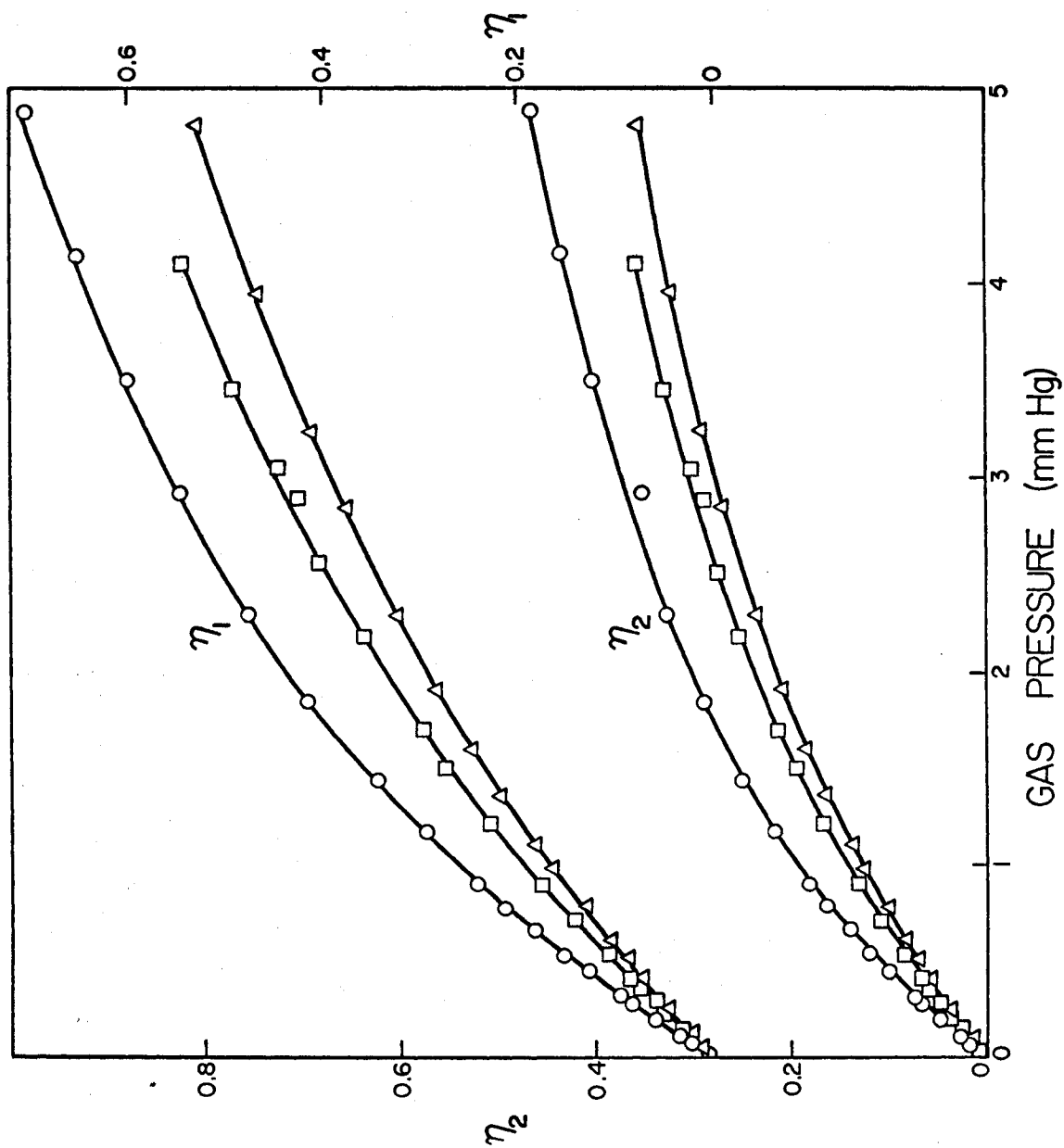


Fig. 13. Plots of intensity ratios η_1 and η_2 against C_2H_6 , CH_4 and CD_4 gas pressures.
 (o) C_2H_6 ; (□) CH_4 ; (Δ) CD_4 .

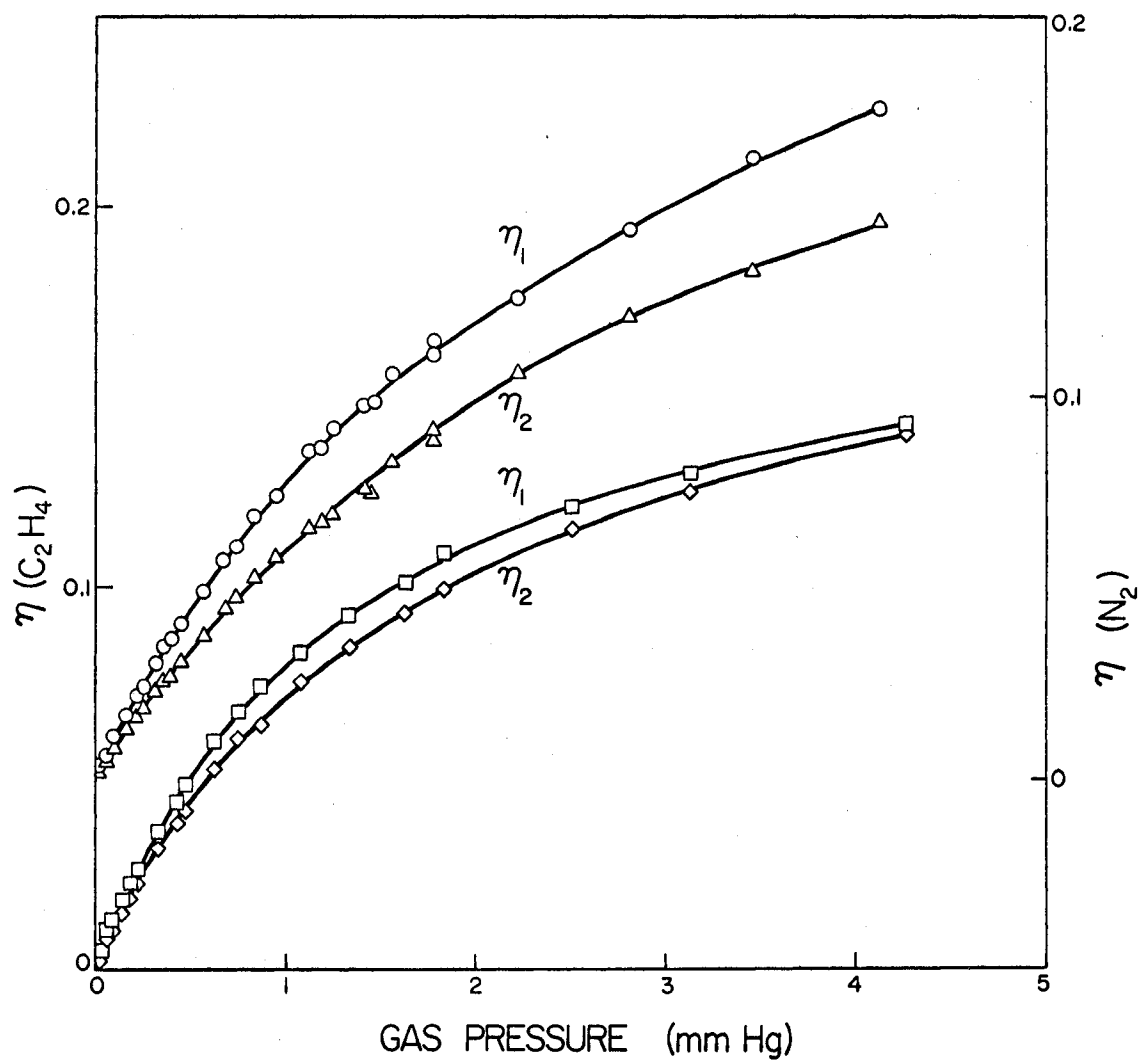


Fig. 14. Plots of intensity ratios η_1 and η_2 against N_2 and C_2H_4 gas pressures.

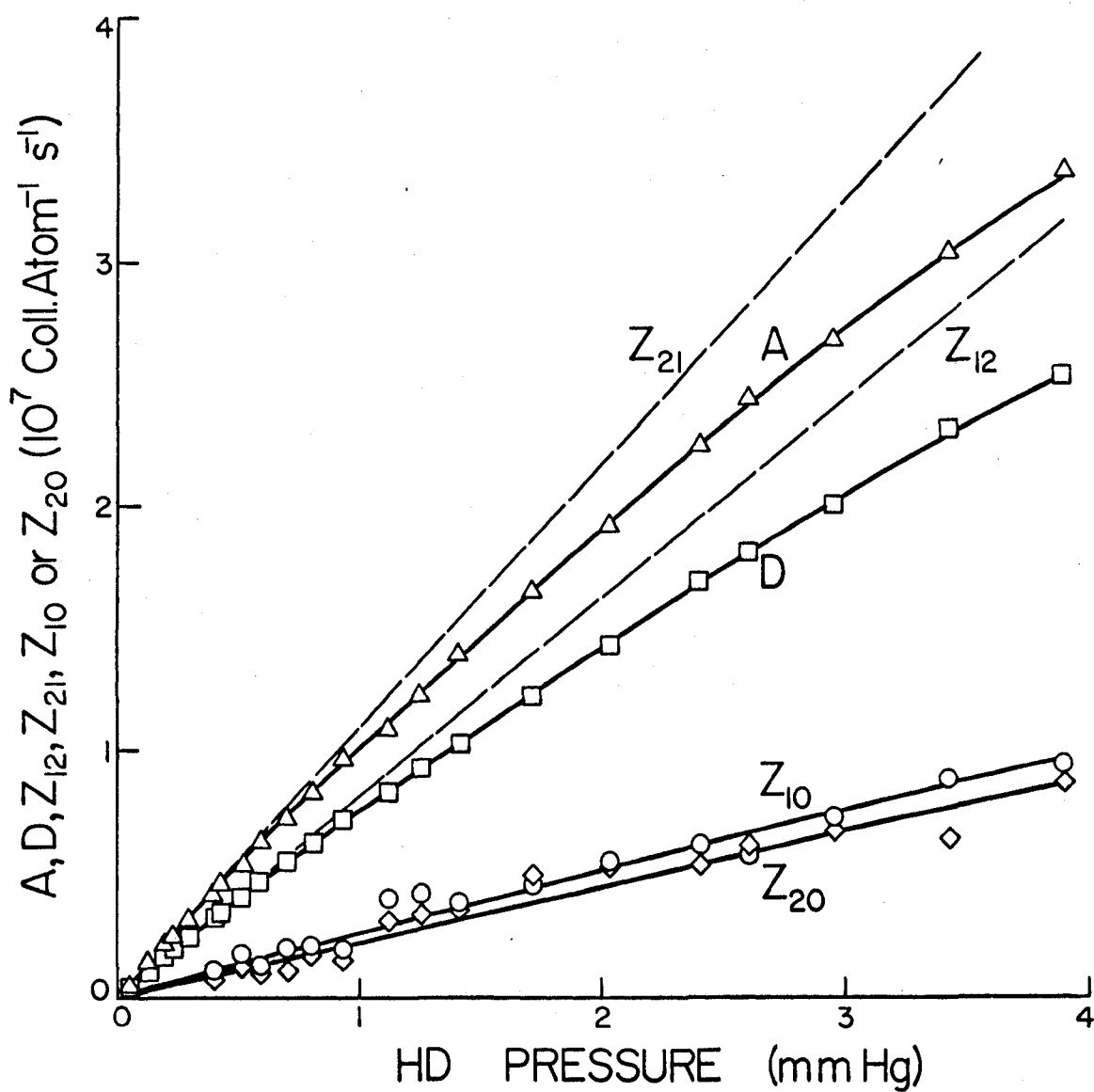


Fig. 15. Plots of collision numbers Z_{12} , Z_{21} , Z_{10} , Z_{20} and the coefficients A and D against HD pressure. The dashed lines Z_{12} and Z_{21} are extrapolations of the straight lines obtained for A and D at low Z_{21} gas pressures where quenching is negligible ($Z_{21} = A$, $Z_{12} = D$).

from linearity indicating that quenching is insignificant compared with the collisional mixing process. The opposite is true, however, with N_2 and C_2H_4 as is shown for N_2 in Fig. 16. In these cases, quenching effects became noticeable at gas pressures as low as 0.25 mm Hg for N_2 and 0.15 mm Hg for C_2H_4 .

The cross sections for collisional mixing and quenching, which were calculated by a least-squares analysis of the Z-P plots, are summarized in Table 2.

B. Discussion of the Results

The statistical uncertainties in the mixing cross sections were negligible in all cases. Uncertainties in the filter transmissions and in the lifetimes of the rubidium resonance states added about 2% each to the error and the pressures read off the McLeod gauge were estimated accurate to within 3%. The combined errors are not expected to exceed $\pm 10\%$.

The quenching cross sections, which are regarded as being of secondary importance, are not nearly as accurate. In the cases of C_2H_4 and N_2 where statistical uncertainties are small compared to other sources of error such as the uncertainty in the corresponding mixing cross sections, the error is estimated at $\pm 20\%$. For the other molecules, especially the saturated hydrocarbons where quenching effects are very small, large statistical uncertainties in the values of Z_{10} and Z_{20} add substantially to the error.

The cross sections for $^2P_{1/2} \leftrightarrow ^2P_{3/2}$ mixing induced by collisions with molecules are 4-5 orders of magnitude larger than the

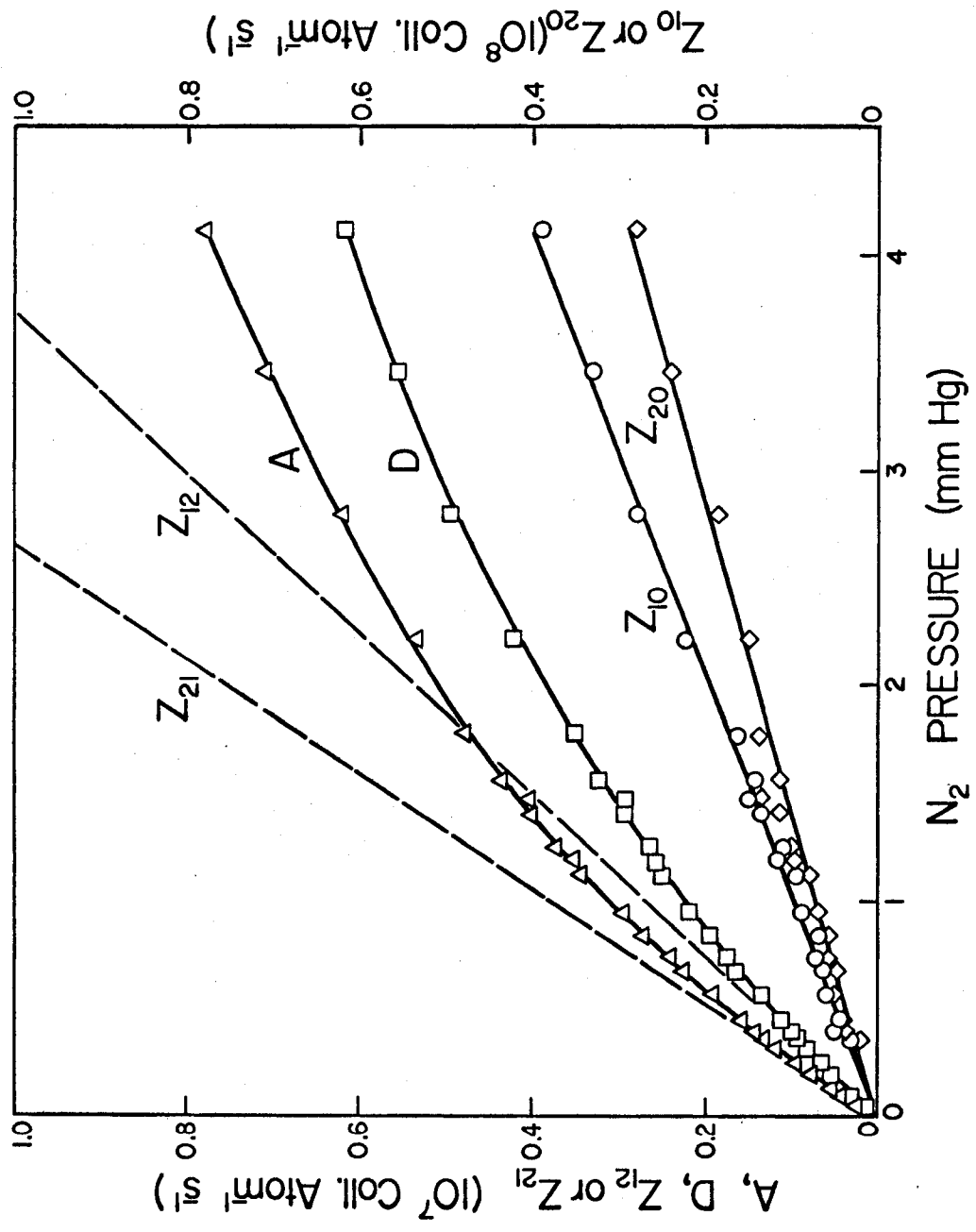


Fig. 16. Plots of collision numbers Z_{12} , Z_{21} , Z_{10} , Z_{20} and the coefficients A and D against N_2 pressure. The dashed lines Z_{12} and Z_{21} are extrapolations of the straight lines obtained for A and D at low gas pressures where quenching is negligible ($Z_{21} = A$, $Z_{12} = D$).

TABLE 2
Cross Sections for Mixing and Quenching in Rb - Molecule Collisions

Collision Partners	Molecular Polarizability $\alpha \times 10^{25}$ (cm^3)	$Q_{12} (^2P_{1/2} \rightarrow ^2P_{3/2})$ (\AA) ²	$Q_{21} (^2P_{1/2} \rightarrow ^2P_{3/2})$ (\AA) ²	$\frac{Q_{12}}{Q_{21}}$	$2 \exp(-\Delta E/kT)$	$Q_{10} (^2P_{1/2} \rightarrow ^2S_{1/2})$ (\AA) ²	$Q_{20} (^2P_{3/2} \rightarrow ^2S_{1/2})$ (\AA) ²
Rb - H ₂	7.9	11	15	0.71	0.72	6 ± 2	3 ± 2
Rb - HD	7.9	18	25	0.74	0.72	6 ± 2	5 ± 2
Rb - D ₂	7.9	22	30	0.75	0.72	3 ± 1	5 ± 2
Rb - N ₂	17.6	16	23	0.73	0.72	58 ± 12	43 ± 11
Rb - CH ₄	26.0	30	42	0.73	0.72	< 1	3 ± 2
Rb - CD ₄	26.0	28	38	0.73	0.72	2 ± 2	3 ± 3
Rb - C ₂ H ₄	42.6	23	32	0.74	0.72	139 ± 28	95 ± 21
Rb - C ₂ H ₆	44.7	57	77	0.74	0.72	2 ± 2	6 ± 3

corresponding cross sections for rubidium - inert gas collisions (Pitre, Rae and Krause 1966). Evidence of the existence of metastable N_2^- ions (Schulz 1964) has given support to the suggestion that the collisional mixing induced with diatomic molecules may proceed according to a mechanism involving an intermediate ionic complex. Calculations based on this assumption, carried out for a Rb - N_2 system by Andreev and Voronin (1969), have yielded cross sections in good agreement with the experimental results as may be seen in Table 3. The experimental value quoted by Bellisio, Davidovits and Kindlmann (1968), although in better agreement with the theoretical prediction, represents only an estimate of the mixing cross section Q_{21} which was used by the authors as a small correction to the quenching cross section Q_{20} .

The large mixing cross sections for collisions of rubidium with H_2 , HD and D_2 may be due to the close correspondence between the separations of the molecular rotational levels and the rubidium 2P_J energy defect (238 cm^{-1}). In fact, the mixing cross sections for the respective isotopes were found to be inversely proportional to their rotational constants 'B', and thus proportional to the spacing between the rotational levels whose term values are given by

$$F(J) = BJ(J + 1)$$

where $F(J)$ is the rotational term in units of cm^{-1} and J is the rotational quantum number. It is difficult to speculate whether the differences in the respective cross sections can be attributed to any particular resonance between the $^2P_{1/2} - ^2P_{3/2}$ energy defect in

TABLE 3

Cross Sections for Mixing and Quenching in Rb - H₂ and Rb - N₂ Systems

Collision Partners	Source	$Q_{21}(^2P_{1/2} \leftarrow ^2P_{3/2})$ (Å) ²	$Q^*(^2S_{1/2} \leftarrow ^2P_{1/2}, ^2P_{3/2})$ (Å) ²	T (°K)
Rb - N ₂	This Investigation	23	50 ± 12	340
	Bellisio, Davidovits and Kindlmann (1968)	7	36 ± 4	304
	Jenkins (1968)		6.1 ± 0.6	1400
	Hooymayers and Nienhuis (1968)		25 ± 1.5	1900
	Andreev and Voronin (1969)	8		300
Rb - H ₂	This Investigation	15	4.5 ± 2	340
	Jenkins (1968)		0.61 ± .1	1400
	Hooymayers and Nienhuis (1968)		3.6 ± 0.4	1900

* Q is the average of Q₁₀ and Q₂₀.

rubidium and a molecular rotational transition, but it appears that the greater the number of rotational transitions available with energies corresponding closely to the 2P_J energy defect, the larger the cross sections. It was noted by McGillis and Krause (1968b) that in collisions of cesium with H_2 , HD and D_2 , the cross sections increased from D_2 to H_2 , exactly the reverse of which has been observed here for rubidium. In cesium, however, the 2P_J energy defect (554 cm^{-1}) corresponds much more closely to the larger energies of the rotational transitions in H_2 whereas in rubidium there is a closer correspondence with transitions in D_2 . In collisions of sodium and potassium with H_2 , HD and D_2 which were studied by Stupavsky and Krause (1968), and McGillis and Krause (1968a), respectively, where the 2P_J energy defects are too small to produce rotational excitation, the energy ΔE is probably converted to translational energy as in alkali-inert gas collisions. It was found in these cases, that the mixing cross sections were almost equal for the various isotopes. Since the internal molecular structure appears not to be a significant factor, and since it is expected that the interaction forces between an alkali atom and the various isotopes of hydrogen are identical, the differences between the mixing cross sections measured at constant temperature, can likely be ascribed to the velocity dependence of the cross sections. Gallagher (1968) has shown a strong velocity (temperature) dependence to exist in rubidium or cesium - inert gas collision cross sections where the collisions are becoming more sudden (more non-adiabatic) as the relative velocity between colliding partners increases. In the present case, the existence of internal molecular

structure complicates the interpretation. If the mixing process proceeded through a long lived intermediate complex, the differences in the respective mixing cross sections for rubidium with the various isotopes of hydrogen might be partially explained by relating the cross sections to the stretching frequencies of the molecular vibrational modes (Melander 1960). McGillis and Krause (1969), who studied the temperature dependence of the mixing cross sections for collisions of excited cesium atoms with CH_4 and CD_4 , accounted for the different temperature dependence of the mixing cross sections observed in the two systems by assuming this type of isotope effect on the collisional rates. In the present experiment, the mixing cross sections for $\text{Rb} - \text{CH}_4$ and $\text{Rb} - \text{CD}_4$ systems were found to be equal within experimental error at a temperature of 340°K , at which the $\text{Cs} - \text{CH}_4$ and $\text{Cs} - \text{CD}_4$ cross sections were found equal by McGillis and Krause (1969).

The saturated hydrocarbons CH_4 , CD_4 and C_2H_6 appear to behave similarly to the inert gases, in that the quenching cross sections are small and the mixing cross sections increase with the molecular polarizabilities. This behaviour was observed for collisions with sodium (Stupavsky and Krause 1969) where the experimental results were found to be in agreement with calculations based on a theory developed for alkali - inert gas collisions by Callaway and Bauer (1965), in which a Van der Waals interaction potential was assumed. Since this theory is applicable only to the non-adiabatic case where the 2P_J energy defect can be neglected, no comparison between experimental and calculated cross sections is possible.

As mentioned previously, the values of the quenching cross

sections are considered to be the least reliable. The observed quenching cross sections for H_2 , HD and D_2 are substantially smaller than those observed with nitrogen where the large cross sections have been attributed to the relatively easy formation of the Rb - N_2 ionic transition complex caused by potential unsaturation in nitrogen (Kibble, Copley and Krause 1967). The cross sections for collisions with nitrogen and hydrogen are compared with some recent determinations of other authors in Table 3. The cross sections Q_{10} and Q_{20} for all the molecular gases were found to be equal within experimental error and there was no evidence of a resonance effect between the rubidium transitions $^2S_{1/2} \leftarrow ^2P_{1/2}$, $^2P_{3/2}$ and vibrational transitions in the diatomic molecules H_2 , HD, D_2 and N_2 , such as were found by Hooymayers and Nienhuis (1968), whose measurements of quenching cross sections for collisions between alkali atoms and diatomic molecules at flame temperatures showed a direct correspondence between increasing magnitudes of the cross sections and the diminishing energy gaps between the alkali fine structure levels and the nearest molecular vibrational levels. It should be noted that no allowance is made in the present study for any chemical reactions that may occur between excited rubidium atoms and ground state molecules. Any such reaction might account for the fact that quenching cross sections measured in flames, where the high temperatures prevent the formation of chemical compounds, are generally smaller than those measured at lower temperatures. It is quite likely, for example, that the large quenching cross sections observed with the Rb - C_2H_4 system arise from rubidium

adding to the double bond of C_2H_4 and forming free radicals which could subsequently polymerize.

VII. CONCLUSIONS

A. Transfer of Excitation in Potassium - Rubidium Collisions

The experimental cross sections for the collisional processes occurring in K - Rb vapour mixtures were found to agree within an order of magnitude with the values calculated by Dashevskaya et al (1970) who developed the first theoretical treatment of excitation transfer in collisions between dissimilar alkali atoms. Previous theoretical work involving transfer of excitation in alkali - alkali collisions had been restricted to collisions between identical atoms (Dashevskaya, Voronin and Nikitin 1969).

Since the cross sections for excitation transfer from one species of alkali atoms to another are relatively small, the sensitized fluorescence, when measured at the low vapour densities required to avoid radiation imprisonment, is difficult to observe. On the other hand, the cross sections for mixing in potassium induced in collisions with ground state rubidium atoms are much larger as are the observed signals at the appropriate vapour densities. This fact should provide a good opportunity to verify further the theory of Dashevskaya et al (1970). In the experimental determination of the cross sections for mixing in, for example, sodium induced by collisions with other alkali atoms, only the fluorescence emitted by the sodium atoms need be observed. This being the case, the vapour densities of only the sodium atoms, which are initially excited, must be kept low and, in

this way, it should be possible to obtain accurate cross sections for mixing in sodium, induced in collisions with the other alkali atoms (potassium, rubidium and cesium).

B. Transfer of Excitation in Collisions Between Rubidium Atoms and Gas Molecules

As in the case of collisions between cesium and gas molecules (McGillis and Krause 1968b, 1969), the cross sections for mixing in rubidium induced by molecular gases were about four orders of magnitude larger than the corresponding cross sections for rubidium - inert gas collisions. This is not surprising since gas molecules possess a comparatively complex internal structure which provides more channels which can accept the energy difference between the 2P_J components of the resonance doublet. The role of the internal molecular structure in the energy transfer process is still not clear. The cross sections observed here for rubidium and those observed by McGillis and Krause (1968b) for cesium, in both of which the mixing was induced in collisions with the various isotopes of hydrogen, indicate that the excitation transfer process is greatly enhanced if the splitting between the rotational levels corresponds closely to the energy separation of the alkali 2P_J substates. No evidence was found however to suggest the possibility of a resonance effect. McGillis and Krause (1969) and later Walentynowicz, Phaneuf and Krause (1970), have been able to relate the mixing cross sections observed for cesium in collisions with polyatomic molecules, to the molecular vibrational frequencies. Although the energy involved is too small to directly

excite the molecular vibrations, the molecules generally vibrate several times during the collision time ($\sim 10^{-13}$ sec). This vibration may be instrumental in inducing the mixing. Further experiments which are now in progress should add insight into the excitation transfer mechanism.

C. Quenching of Rubidium Resonance Radiation by Collisions with Molecules

The diatomic molecules H_2 , HD, D_2 and N_2 , as well as the unsaturated polyatomic molecule C_2H_4 , are more efficient quenchers than the saturated hydrocarbons CH_4 , CD_4 and C_2H_6 , which were found to behave similarly to the inert gases. If it is assumed that the quenching reaction proceeds through an ionic complex (Andreev and Voronin 1969), then the quenching rates must depend on the ease with which the ionic complex is formed. Hence, the quenching of excited states by inert gases, where the electron affinities are virtually zero (Herzberg 1944), is expected to be much less effective than that observed with diatomic molecules.

The quenching cross sections for H_2 , HD and D_2 were not found to be significantly different to suggest any resonance effect between the rubidium resonance levels and the molecular vibrational levels which are quite different for the various isotopes of hydrogen. Even when the quenching cross sections obtained with the isotopes of hydrogen were compared to the much larger values obtained with nitrogen, no evidence of a resonance was established. If a resonance effect did, indeed, exist, the observed cross sections should be quite sensitive as to which rubidium substate was initially excited. The quenching

cross sections obtained here were not considered accurate enough to suggest any such differences.

Quenching cross sections obtained at flame temperatures (2000°K) are significantly smaller than those obtained here and in other investigations at similar temperatures ($300 - 400^{\circ}\text{K}$). If the colliding molecules are chemically reactive, the formation of a stable complex through which the quenching reaction may proceed is greatly enhanced. However, at the high temperatures found in flames, the large energies of dissociation inhibit the formations of such complexes. Hooymayers and Alkemade (1966), who plotted the cross sections for quenching of excited sodium atoms in collisions with nitrogen molecules at various relative velocities of the colliding species as determined by various investigators, have also found a fairly complex velocity dependence of the cross sections. It has recently become apparent from results of atomic beam experiments (Anderson, Aquilanti and Herschbach 1969), that cross sections for excitation of potassium atoms induced in collisions with a particular target gas (the inverse of quenching) depend strongly on the relative energy of the colliding partners. The beam experiments, however, do not extend to low enough energies to provide a direct comparison with the quenching cross sections.

APPENDIX A

EXPERIMENTAL MEASUREMENTS
OF THE
EXTINCTION COEFFICIENTS
AND
FLUORESCENT INTENSITY RATIOS
IN
K - Rb VAPOUR MIXTURES

Extinction Coefficients β in Pure Rubidium Vapour for
the 7948 Å Component of the Resonance Doublet

Side Oven Temperature (°C)	β (cm ⁻¹)	Side Oven Temperature (°C)	β (cm ⁻¹)
44.3	.117	63.4	.535
46.8	.156	64.0	.602
49.6	.177	64.1	.592
50.4	.189	67.0	.742
50.7	.196	67.5	.751
52.4	.249	68.8	.843
53.5	.277	68.8	.825
56.2	.352	69.1	.898
58.0	.363	71.3	.980
58.9	.402	73.5	1.10
61.5	.488	76.0	1.22
61.6	.460	77.5	1.32
63.0	.545	80.8	1.40

Extinction Coefficients β for the Resonance Lines of
Rubidium in K - Rb Vapour Mixtures

Side Oven Temperature (°C)	β (7800 Å) (cm ⁻¹)	β (7948 Å) (cm ⁻¹)
67.1	.602	.296
69.6	.751	.344
72.2	.816	.440
74.4	.953	.497
76.0	1.02	.583
78.0	1.11	.705
79.8	1.29	.797
82.6	1.46	.861
84.6	1.49	.980
85.8	1.58	1.06
88.3	1.75	1.23
89.9	1.83	1.33
92.4	1.96	1.40
94.4	1.97	1.48
96.2	2.11	1.55
98.6	2.08	1.66
101.0	2.21	1.76
104.0	2.36	1.86
106.6	2.41	2.03
109.4	2.46	2.08
112.3	2.56	2.22
115.1	2.60	2.26

Extinction Coefficients β for the Resonance Lines of
Potassium in K - Rb Vapour Mixtures

Side Oven Temperature ($^{\circ}\text{C}$)	β (7665 \AA) (cm^{-1})	β (7699 \AA) (cm^{-1})
76.3	.266	
80.0	.334	
83.6	.488	.225
86.8	.583	.320
90.7	.770	.383
94.3	.944	.535
97.7	1.14	.667
100.5	1.33	.825
104.4	1.54	1.02
107.6	1.78	1.21
110.9	1.96	1.41
114.8	2.11	1.61

Fluorescent Intensity Ratios in K - Rb Vapour Mixtures
(Corrected for Reabsorption)

P_1 (Rb) (10^{-5} mm Hg)	η_{12} (10^{-6})	P_1 (Rb) (10^{-5} mm Hg)	η_{12} (10^{-6})
.475	1.48	5.54	8.40
.800	3.10	6.17	9.36
1.03	3.75	6.55	9.96
1.27	3.15	7.41	10.9
1.39	3.20	7.41	12.4
1.60	3.88	8.30	13.3
1.85	3.47	8.75	14.4
2.24	4.04	9.39	15.4
2.77	4.14	10.4	17.3
3.22	4.93	11.4	20.4
3.85	5.69	12.2	22.7
4.04	5.75	14.2	27.3
4.53	6.57	15.8	34.8
5.01	7.43	18.3	41.3

P_1 (Rb) (10^{-5} mm Hg)	η_{22} (10^{-6})	P_1 (Rb) (10^{-5} mm Hg)	η_{22} (10^{-6})
.516	.328	2.75	2.98
.718	.772	3.03	3.44
.942	.843	3.14	3.93
1.16	1.26	3.55	4.79
1.42	1.14	4.30	6.95
1.61	1.21	5.46	10.6
1.70	1.04	6.92	16.4
1.87	1.58	8.60	22.9
2.06	1.83	10.2	33.1
2.39	2.28	11.8	43.7
2.50	2.84	13.8	56.8

P_1 (Rb) (10^{-5} mm Hg)	η_{11} (10^{-6})	P_1 (Rb) (10^{-5} mm Hg)	η_{11} (10^{-6})
5.72	.591	11.4	1.30
6.88	.797	11.7	1.36
8.04	.789	12.5	1.42
8.68	.862	13.3	1.62
9.01	.932	14.0	1.88
9.28	.894	15.9	1.99
9.99	1.05	19.1	2.95
10.7	1.13		

P_1 (Rb) (10^{-5} mm Hg)	η_{21} (10^{-6})	P_1 (Rb) (10^{-5} mm Hg)	η_{21} (10^{-6})
2.82	.379	6.40	.997
3.50	.364	6.47	1.02
4.04	.428	6.84	1.03
4.49	.444	7.52	1.07
4.56	.550	8.04	1.39
4.94	.693	9.01	1.41
5.20	.587	9.87	1.92
5.46	.747	11.1	2.34
5.80	.833	13.2	3.07
5.91	.872		

P_1 (Rb) (10^{-5} mm Hg)	η_1 (10^{-5})	η_1'' (10^{-5})
1.18	.850	.614
1.64	1.43	1.11
1.79	1.76	1.41
2.24	1.87	1.42
2.53	2.36	1.84
2.67	2.18	1.63
2.89	2.68	2.08
3.27	2.82	2.14
3.64	3.05	2.28
4.07	3.72	2.84
4.26	3.78	2.85
4.70	4.41	3.37
5.18	4.73	3.57
5.22	5.72	4.52
5.85	5.68	4.36
6.40	7.80	6.26
6.85	8.40	6.76
7.03	8.50	6.81
7.51	10.3	8.40
8.03	11.0	8.97
8.66	13.1	10.9
9.80	16.8	14.7

P_1 (Rb) (10^{-5} mm Hg)	η_2 (10^{-5})	η_2'' (10^{-5})
.918	1.14	.892
1.25	1.21	.867
1.81	2.16	1.69
2.14	2.64	2.09
2.50	3.07	2.41
3.00	3.90	3.10
3.26	4.13	3.27
3.64	4.64	3.68
4.03	5.13	4.06
4.26	4.95	3.78
4.55	6.21	4.97
4.74	6.48	5.22
5.00	6.56	5.21
5.29	6.62	5.19
5.64	7.62	6.08
6.11	9.27	7.64
6.22	8.65	6.98
7.07	10.4	8.50
7.25	12.2	10.3
7.92	12.3	10.2
8.44	14.0	11.8
9.44	17.3	15.0
9.84	18.8	16.3
11.1	21.8	19.1

APPENDIX B

EXPERIMENTAL DATA

FOR

RUBIDIUM-MOLECULAR GAS COLLISIONS

Rb - H₂ DATA

P (mm Hg)	η_1	η_2
.0095	.00190	.00147
.016	.00341	.00256
.018	.00386	.00290
.033	.00752	.00565
.037	.00792	.00593
.037	.00796	.00615
.056	.0126	.00953
.076	.0169	.0127
.091	.0192	.0146
.110	.0240	.0183
.121	.0268	.0202
.129	.0280	.0210
.193	.0399	.0299
.234	.0496	.0377
.245	.0534	.0396
.417	.0813	.0627
.462	.875	.0673
.568	.106	.0816
.650	.123	.0947
.658	.120	.0920
.697	.128	.0995
.904	.155	.119
1.02	.181	.136
1.08	.185	.140
1.21	.200	.150
1.34	.218	.166
1.48	.231	.175
1.50	.226	.171
1.67	.257	.193
1.68	.253	.194
1.79	.265	.203
1.96	.284	.216
2.19	.305	.238
2.45	.327	.251
3.03	.374	.279
3.31	.386	.295
4.21	.430	.327
4.62	.463	.340

Rb - HD DATA

P (mm Hg)	η_1	η_2
.0091	.00245	.00214
.015	.00425	.00343
.033	.00948	.00750
.043	.0120	.0959
.050	.0140	.0111
.059	.0167	.0132
.074	.0208	.0163
.096	.0269	.0212
.106	.0307	.0236
.131	.0378	.0287
.158	.0448	.0359
.198	.0554	.0446
.231	.0629	.0507
.296	.0792	.0640
.401	.104	.823
.433	.112	.868
.516	.128	.102
.592	.147	.115
.698	.167	.132
.807	.188	.147
.930	.214	.165
1.12	.237	.185
1.25	.258	.200
1.41	.286	.217
1.71	.326	.244
2.03	.364	.271
2.40	.405	.302
2.60	.430	.314
2.95	.455	.335
3.42	.489	.366
3.89	.524	.381

Rb - D₂ DATA

P (mm Hg)	η_1	η_2
.0075	.00200	.00161
.0087	.00242	.00198
.016	.00438	.00349
.028	.00829	.00659
.033	.00968	.00770
.037	.0110	.00869
.051	.0156	.0123
.061	.0187	.0148
.073	.0215	.0168
.109	.0327	.0257
.128	.0379	.0301
.171	.0507	.0417
.215	.0639	.0505
.285	.0824	.0657
.329	.0930	.0730
.479	.129	.102
.586	.155	.121
.744	.191	.147
.896	.221	.170
1.12	.260	.193
1.26	.291	.213
1.52	.329	.243
1.76	.357	.264
1.97	.395	.290
2.42	.450	.317
2.72	.480	.343
3.32	.553	.375
4.17	.604	.414
4.95	.651	.441

Rb - N₂ DATA

P (mm Hg)	η_1	η_2
.0085	.000887	.000669
.014	.00158	.00114
.020	.00218	.00161
.026	.00267	.00198
.027	.00267	.00210
.033	.00353	.00260
.035	.00342	.00268
.036	.00371	.00264
.038	.00403	.00293
.044	.00489	.00355
.054	.00596	.00436
.063	.00677	.00496
.067	.00725	.00535
.069	.00755	.00546
.073	.00753	.00541
.074	.00791	.00575
.083	.00798	.00634
.085	.00930	.00673
.106	.0112	.00807
.120	.0126	.00946
.135	.0141	.0107
.165	.0166	.0126
.201	.0198	.0150
.204	.0202	.0155
.218	.0218	.0164
.256	.0241	.0180
.276	.0247	.0193
.323	.0303	.0226
.364	.0345	.0253
.385	.0346	.0257
.401	.0364	.0264
.452	.0404	.0304
.458	.0411	.0315
.569	.0487	.0366
.592	.0508	.0390
.678	.0568	.0442
.742	.0606	.0467
.837	.0685	.0523
.950	.0740	.0576
1.12	.0857	.0656
1.19	.0868	.0670
1.25	.0919	.0688
1.29	.0884	.0688
1.31	.0907	.0741

Rb - N₂ DATA (continued)

P (mm Hg)	η_1	η_2
1.41	.0981	.0756
1.47	.0986	.0749
1.56	.106	.0826
1.77	.111	.0916
1.78	.115	.0889
2.21	.126	.106
2.80	.144	.121
3.45	.163	.133
4.12	.176	.146

Rb - CH₄ DATA

P (mm Hg)	η_1	η_2
.011	.00244	.00192
.016	.00385	.00307
.022	.00516	.00416
.028	.00670	.00535
.035	.00860	.00670
.044	.0106	.00825
.053	.0125	.0100
.060	.0145	.0113
.072	.0171	.0133
.083	.0193	.0153
.108	.0255	.0196
.127	.0292	.0230
.154	.0347	.0278
.232	.0511	.0388
.285	.0601	.0480
.347	.0754	.0588
.400	.0867	.0674
.522	.110	.0847
.705	.145	.109
.895	.175	.132
1.21	.230	.168
1.50	.276	.194
1.70	.297	.214
2.19	.359	.254
2.56	.404	.275
2.89	.426	.291
3.05	.446	.304
3.45	.492	.330
4.10	.544	.360

Rb - CD₄ DATA

P (mm Hg)	η_1	η_2
.0092	.00184	.00152
.019	.00360	.00274
.031	.00621	.00511
.043	.00811	.00657
.045	.00879	.00731
.052	.0100	.00824
.060	.0120	.00964
.076	.0150	.0116
.086	.0161	.0130
.093	.0184	.0149
.118	.0235	.0181
.145	.0269	.0212
.174	.0338	.0262
.188	.0341	.0272
.251	.0473	.0370
.304	.0543	.0423
.320	.0615	.0480
.407	.0749	.0575
.508	.0875	.0680
.600	.107	.0820
.780	.130	.101
.815	.128	.106
.980	.165	.125
1.10	.182	.135
1.36	.220	.163
1.60	.247	.185
1.91	.283	.208
2.29	.324	.235
2.84	.375	.270
3.24	.412	.292
3.95	.467	.324
4.82	.530	.358

Rb - C₂H₄ DATA

P (mm Hg)	η_1	η_2
.0042	.000617	.000510
.010	.00146	.00116
.022	.00313	.00250
.033	.00460	.00376
.040	.00566	.00466
.045	.00633	.00500
.055	.00747	.00597
.063	.00883	.00708
.073	.0101	.00803
.096	.0128	.0104
.116	.0155	.0125
.139	.0179	.0145
.179	.0225	.0181
.226	.0265	.0228
.331	.0367	.0317
.418	.0441	.0383
.478	.0485	.0419
.626	.0598	.0528
.756	.0674	.0607
.876	.0736	.0642
1.08	.0827	.0752
1.34	.0926	.0844
1.63	.101	.0933
1.83	.109	.101
2.12	.111	.109
2.51	.121	.115
3.12	.130	.125
3.74	.134	.130
4.26	.143	.141

Rb - C₂H₆ DATA

P (mm Hg)	η_1	η_2
.0061	.00210	.00166
.017	.00583	.00454
.024	.00833	.00644
.037	.0129	.0101
.052	.0179	.0141
.070	.0237	.0185
.089	.0298	.0232
.109	.0352	.0275
.136	.0447	.0347
.195	.0610	.0489
.271	.0850	.0667
.309	.0968	.0752
.436	.129	.101
.529	.155	.119
.656	.184	.141
.777	.214	.165
.896	.243	.182
1.17	.295	.217
1.44	.344	.251
1.85	.415	.290
2.30	.476	.329
2.92	.547	.374
3.50	.603	.404
4.15	.651	.435
4.89	.707	.468

BIBLIOGRAPHY

1. Anderson, R. W., Aquilanti, V. and Herschbach, D. R. 1969. Chem. Phys. Letters 4, 5.
2. Andreev, E. A. and Voronin, A. I. 1969. Chem. Phys. Letters 3, 488.
3. Atkinson, R., Chapman, G. D. and Krause, L. 1965. J. Opt. Soc. Am. 55, 1269.
4. Bellisio, J. A., Davidovits, P. and Kindlmann, P. J. 1968. J. Chem. Phys. 48, 2376.
5. Bennewitz, H. G. and Dohmann, H. D. 1965. Z. Physik, 182, 524.
6. Callaway, J. and Bauer, E. 1965. Phys. Rev. 140, A1072.
7. Chapman, G. D. 1965. Ph.D. Thesis, University of Windsor, Windsor, Ontario.
8. Chapman, G. D. and Krause, L. 1965. Can. J. Phys. 44, 753.
9. Copley, G. and Krause, L. 1969. Can. J. Phys. 47, 533.
10. Czajkowski, M., McGillis, D. A. and Krause, L. 1966a. Can. J. Phys. 44, 91.
11. Czajkowski, M., McGillis, D. A. and Krause, L. 1966b. Can. J. Phys. 44, 741.
12. Dashevskaya, E. I., Nikitin, E. E., Voronin, A. I. and Zembekov, A. A. 1970. Can. J. Phys. (to be published).
13. Dashevskaya, E. I., Voronin, A. I. and Nikitin, E. E. 1969. Can. J. Phys. 47, 1237.

14. Dushman, S. and Lafferty, J. M. 1962. Scientific Foundations of Vacuum Technique (John Wiley and Sons Inc., New York).
15. Friedrich, H. and Seiwert, R. 1957. Ann. Physik 20, 215.
16. Gallagher, A. 1968. Phys. Rev. 172, 88.
17. Herzberg, G. 1944. Atomic Spectra and Atomic Structure (Dover Publications, Inc., New York).
18. Hoffmann, K. 1962. Exp. Tech. Phys. 39, 217.
19. Hoffmann, K. and Seiwert, R. 1961. Ann. Physik 7, 71.
20. Hooymayers, H. P. and Alkemade, C. Th. J. 1966. J.Q.S.R.T. 6, 847.
21. Hooymayers, H. P. and Nienhuis, G. 1968. J.Q.S.R.T. 8, 955.
22. Hrycyshyn, E. S. and Krause, L. 1969a. Can. J. Phys. 47, 215.
23. Hrycyshyn, E. S. and Krause, L. 1969b. Can. J. Phys. 47, 223.
24. Hudson, B. C. and Curnutte, B. Jr., 1966. Phys. Rev. 152, 56.
25. Jenkins, D. R. 1968. Proc. Roy. Soc. A. 303, 453.
26. Kibble, B. P., Copley, G. and Krause, L. 1967. Phys. Rev. 153, 9.
27. Kraulinya, E. K. 1964. Opt. Spectrosk. 17, 464. (English Trans.: 1966. Opt. Spectry. (U.S.S.R.) 17, 250.)
28. Kraulinya, E. K. and Lezdin, A. E. 1966. Opt. Spectrosk. 20, 539. (English Trans.: 1966. Opt. Spectry. (U.S.S.R.) 20, 304.)
29. Link, J. K. 1966. J. Opt. Soc. Am. 56, 1195.
30. McGillis, D. and Krause, L. 1968a. Can. J. Phys. 46, 25.
31. McGillis, D. and Krause, L. 1968b. Can. J. Phys. 46, 1051.
32. McGillis, D. and Krause, L. 1969. Can. J. Phys. 47, 473.
33. Melander, L. 1960. Isotope Effects on Reaction Rates (The Ronald Press Co., New York).

34. Mitchell, A. C. G. and Zemansky, M. W. 1961. Resonance Radiation and Excited Atoms (Cambridge University Press, New York).
35. Nesmeyanov, A. N. 1963. Vapor Pressure of the Elements (Academic Press Inc., New York).
36. Ornstein, M. H. and Zare, R. N. 1969. Phys. Rev. 181, 214.
37. Pitre, J. and Krause, L. 1967. Can. J. Phys. 45, 2671.
38. Pitre, B., Rae, A. G. A. and Krause, L. 1966. Can. J. Phys. 44, 731.
39. Rae, A. G. A. and Krause, L. 1965. Can. J. Phys. 43, 1574.
40. Rozwadowski, M. and Lipworth, E. 1966. J. Chem. Phys. 43, 2347.
41. Seiwert, R. 1956. Ann. Physik 18, 54.
42. Shulz, G. L. 1964. Phys. Rev. 135A, 988.
43. Sosinskii, M. L. and Morosov, E. N. 1965. Opt. Spektrosk. 19, 634.
(English Trans.: 1965. Opt. Spectry. (U.S.S.R.) 19, 352.)
44. Stacey, V. and Zare, R. N. 1970. Phys. Rev. (to be published).
45. Stupavsky, M. and Krause, L. 1968. Can. J. Phys. 46, 2127.
46. Stupavsky, M. and Krause, L. 1969. Can. J. Phys. 47, 1249.
47. Thangaraj, M. A. 1948. Ph.D. Thesis, University of Toronto,
Toronto, Ontario.
48. Walentynowicz, E., Phaneuf, R. and Krause, L. 1970. Bull. Am.
Phys. Soc. (to be published).

VITA AUCTORIS

I was born on January 21, 1941 in Kirkland Lake, Ontario where I attended primary and secondary schools. Upon graduation in 1959, I attended the University of St. Michael's College in Toronto, where I graduated in 1963 from a General Science course with a mathematics major. In 1963, I registered as a special student in Arts and Science at the University of Windsor and in 1964 enrolled in the Faculty of Graduate Studies to work toward a Master Degree in Physics which was awarded in 1966. In the past several years, I have held either a Province of Ontario Graduate Fellowship or a National Research Council Bursary.